materials

MDPI

Review

A Comparative Mini-Review on Transition Metal Oxides Applied for the Selective Catalytic Ammonia Oxidation (NH_3-SCO)

Magdalena Jabłońska * and Alejandro Mollá Robles

Institute of Chemical Technology, Universität Leipzig, Linnéstr. 3, 04103 Leipzig, Germany; alejandro.molla_robles@uni-leipzig.de

* Correspondence: magdalena.jablonska@uni-leipzig.de

Abstract: The selective catalytic oxidation of NH_3 (NH_3-SCO) into N_2 and H_2O is an efficient technology for NH_3 abatement in diesel vehicles. However, the catalysts dedicated to NH_3-SCO are still under development. One of the groups of such catalysts constituted transition metal-based catalysts, including hydrotalcite-derived mixed metal oxides. This class of materials is characterized by tailored composition, homogenously dispersed mixed metal oxides, exhibiting high specific surface area and thermal stability. Thus, firstly, we give a short introduction to the structure and composition of hydrotalcite-like materials and their applications in NH_3-SCO. Secondly, an overview of other transition metal-based catalysts reported in the literature is given, following a comparison of both groups. The challenges in NH_3-SCO applications are provided, while the reaction mechanisms are discussed for particular systems.

Keywords: selective ammonia oxidation; hydrotalcite-like compounds; mixed metal oxides; transition metals

Citation: Jabłońska, M.; Mollá Robles, A. A Comparative Mini-Review on Transition Metal Oxides Applied for the Selective Catalytic Ammonia Oxidation (NH_3-SCO). *Materials* **2022**, *15*, 4770. https://doi.org/10.3390/ma15144770

Academic Editor: Yuhang Wang

Received: 29 May 2022
Accepted: 5 July 2022
Published: 7 July 2022

1. Introduction

Ammonia (NH_3) is one of the most important chemicals in the world, e.g., used to produce fertilizers, synthetic fibers, dyes and synthetic foam, as well as to reduce NO_x emissions, etc. (Figure 1). However, since 2001, the EU has listed NH_3 as one of the four main types of atmospheric pollutants (among NO_x, SO_2, and non-methane volatile organic compounds (NMVOC)), and has released the EU National Pollutant Discharge Inventory (NECD) every year. Twelve Member States (including, e.g., Germany, France, Austria, etc.), and the United Kingdom need to reduce NH_3 emissions by up to 10% against 2018 levels to attain their 2020 and 2030 emission reduction commitments. Denmark and Lithuania need to reduce emissions by more than 10% [1]. Ammonia emitted from livestock, industrial processes or NH_3 emitted to the atmosphere through either the large-scale usage of fertilizers or gas slippage from the NH_3-SCR-DeNO_x applications can cause serious damage to human health (i.e., to the eyes, throat, nose, etc., if its concentration exceeds 50–100 ppm) [2], and environment (e.g., acidification, formation of haze, Figure 1).

To control the ammonia slip, several different techniques used for the elimination of NH_3 (e.g., adsorption, absorption, catalytic decomposition, etc.) have been applied [3]. However, the selective catalytic oxidation of ammonia into nitrogen and water vapor is an ideal technology for removing NH_3 from O_2-containing waste gases, after the selective catalytic reduction of NO_x by NH_3 (SCR-DeNO_x, by the use of stoichiometric or even excess amount of NH_3) from stationary and mobile sources. Thus, ideally, the residual NH_3 (slip) could be selectively oxidized to N_2 and H_2O (i.e., inert, and non-toxic products, Equation (1). However, the N_2 selectivity is affected by the undesired oxidation of ammonia to N_2O, NO, and NO_2 (Equations (2)–(4)):

$$4NH_3 + 3O_2 \rightarrow 2N_2 + 6H_2O \quad (1)$$

$$2NH_3 + 2O_2 \rightarrow N_2O + 3H_2O \quad (2)$$

$$4NH_3 + 5O_2 \rightarrow 4NO + 6H_2O \quad (3)$$

$$4NH_3 + 7O_2 \rightarrow 4NO_2 + 6H_2O \quad (4)$$

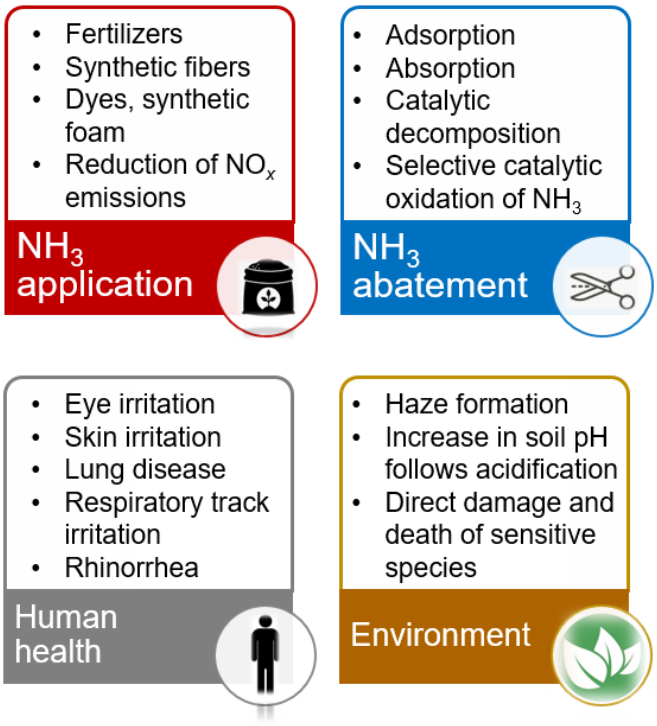

Figure 1. Schematic representation of NH_3 application and abatement, as well as the impact of NH_3 on human health and the environment.

Thus, NH_3-SCO catalysts with enhanced activity, N_2 selectivity, stability (also in the presence of H_2O, SO_x, and CO_x, up to 600–700 °C in the cycle of diesel particulate filter regeneration) and low cost, at the same time are of both scientific and industrial importance. However, catalysts of sufficient activity, selectivity and stability under application-relevant reaction conditions are not yet available. To date, many catalysts have been proposed for NH_3-SCO and they can be classified into several groups, including noble metal-based catalysts, transition metal-based catalysts and noble/transition metal (bimetallic)-containing catalysts, etc. Particularly, the catalysts containing copper species are recognized as the most active and N_2 selective among other transition metal-containing materials. Copper oxide species and their redox properties were found to determine their catalytic properties [4]. Recently, we published on noble metal-based catalysts (including Pt-, Pd-, Ag-, and Au-, Ru-based catalysts) [5] and Cu-containing zeolite-based catalysts (e.g., Cu-SSZ-13 commercialized in NH_3-SCR-DeNO_x) [6]. Thus, in the current mini-review, we focused on the application of transition metal oxides, excluding catalysts modified with noble metals or zeolite-based catalysts. However, the publications and results on the subject of transition metal-based catalysts increased recently, therefore, we found the mini-review timely. Particularly, we aim to compare hydrotalcite-based mixed metal oxides with other transition metal catalysts presented in the literature, and based on that propose an active, N_2 selective, and stable catalytic system (either single one or as a component for hybrid catalyst) for NH_3-SCO. The hybrid catalyst consists of an SCR catalyst for NO_x control and catalyst with oxidation functionality for ammonia conversion. The different arrangements

of the hybrid catalysts, i.e., dual-layer, inverse dual-layer, hybrid dual layer, dual mixed layers, etc., were so far tested in the literature (e.g., [7]). The combination of the two active components for NH_3-SCR-DeNO_x and NH_3 oxidation to yield NO_x arise from the internal selective catalytic reduction mechanism (i-SCR) [3,4]. However, despite research in this direction, a debate remains on the elementary reaction steps and the active sites in NH_3-SCO. Moreover, for the i-SCR mechanism, the imide mechanism (with the formation of imide (-NH) and nitrosyl (-HNO) as intermediates), and the hydrazine mechanism (involving hydrazine (N_2H_4) as an intermediate) are reported as the main mechanisms for NH_3-SCO. Recently, the N_2^- mechanism (with adsorbed N_2 anion regarded as the intermediate), was also proposed to explain the high reactivity of nano-size Al_2O_3-supported Ag species [8]. Contrary to the micro-size Al_2O_3 supported Ag species, the i-SCR mechanism was proposed, evidencing that the reaction mechanism depends on the applied catalytic systems. Another example can constitute Cu species deposited on Al_2O_3. Depending on the applied treatment (calcination *versus* dynamic construction), NH_3-SCO over the catalysts can follow different routes. For example, the fast i-SCR mechanism characterized by the presence of consumable NO_2 adsorbed species was proposed on CuO_x-OH interfacial sites [9]. Still, compared to NH_3-SCR-DeNO_x, the reaction mechanisms of NH_3-SCO are not frequently discussed in the literature. Hence, it is vital to study the reaction mechanisms over more materials thoroughly and then rationally design high-performing NH_3-SCO catalyst with appropriate promotion strategies.

Although some review articles [3,4,10] have outlined the advances of transition-metal-based catalysts in NH_3-SCO, only examples of such materials have been given. Thus, in the current mini-review, we thoroughly discuss the hydrotalcite-derived mixed metal oxides and other transition metal oxides applied in NH_3-SCO, evidencing that for these materials their application as catalysts is quite relevant. Our objective was not to make a systematic review of the hydrotalcite-like compounds because several reviews have already been published, including preparation and physico-chemical characterization (e.g., [11–13]), catalytic applications (e.g., [14,15])—in particular nitrogen oxides removal [16,17]. Despite not being mentioned in the text, selective ammonia oxidation over (mixed) metal oxides into NO [18–22] or N_2O [23,24] was reported, in the present work we concentrate only on the ammonia oxidation into N_2 and H_2O. Throughout the mini-review, we highlight the structure-activity/selectivity correlations and try to narrow the gap between research and industrial applications. We hope that based on these correlations, a knowledge-driven industrial catalyst design and its optimization becomes possible, which will allow keeping the NH_3 emissions of diesel-powered vehicles at a very low level under various boundary conditions.

2. Hydrotalcite-Derived Mixed Metal Oxides

Hydrotalcite-like compounds (HT), otherwise referred to as anionic clays or layered double hydroxides (LDHs) are described by the general formula $[M(II)_{1-x}M(III)_x(OH)_2]^{q+}(A^{n-})_{q/n})$ mH_2O, where M(II) and M(III) represent divalent and trivalent metal cations, respectively, A^{n-} represents interlayer anions of charge n^-. Usually, the structure of the HT-like compounds is better visualized by analyzing the structure of brucite. $Mg(OH)_2$ octahedra of Mg^{2+} coordinated with six OH^- share edges to form successive sheets, with the hydroxide ions located perpendicularly to the plane of the layers. The resulting sheets are stacked on top of each other and held together by hydrogen bonds. When Mg^{2+} ions are substituted by Al^{3+}, a positive charge is created in the hydroxyl part of the layer. The positive charge is neutralized by the negative CO_3^{2-} anions, which are located between the layers of brucite, along with H_2O that is also present in the interlayer space (Figure 2) [25,26]. To obtain a pure hydrotalcite-like phase, the x in the general formula of the material should be in the range of 0.15 and 0.34 [25]. Coprecipitation is the most common method for the synthesis of hydrotalcite-like compounds.

The structure and physico-chemical properties of the hydrotalcite-like compounds are dependent on the kind and amount of metal ions present in the brucite-like layers, the type and position of anions and water in the interlayer region, and the type of stacking between

the layers (i.e., rhombohedral (3R) *versus* hexagonal (2H)) [27]. It is possible to synthesize hydrotalcite-like compounds with more than two different metals (regarding different oxidation states, e.g., Li, Mg, Mn, Fe, Co, Al, Mn, Fe, Co, Ni, Cr, Ga) or anions (halides: Cl^-, F^-, I^-, oxo-anions: CO_3^{2-}, NO_3^-, SO_4^{2-}, BrO_3^-, organic acids: adipic, oxalic, sebacic or malonic acid, oxo and polyoxo-metallates: $(PW_{12}O_{40})^{3-}$, $(PMo_{12}O_{40})^{3-}$, chromate, dichromate, anionic complexes: ferro and ferricyanide, $PdCl_4^{2-}$, etc.). Consequently, the size of the interlayer region varies depending on the introduced anions. e.g., Table 1 lists the products obtained from the preparation of $CuM(II)M(III)CO_3$ hydrotalcite-like compounds.

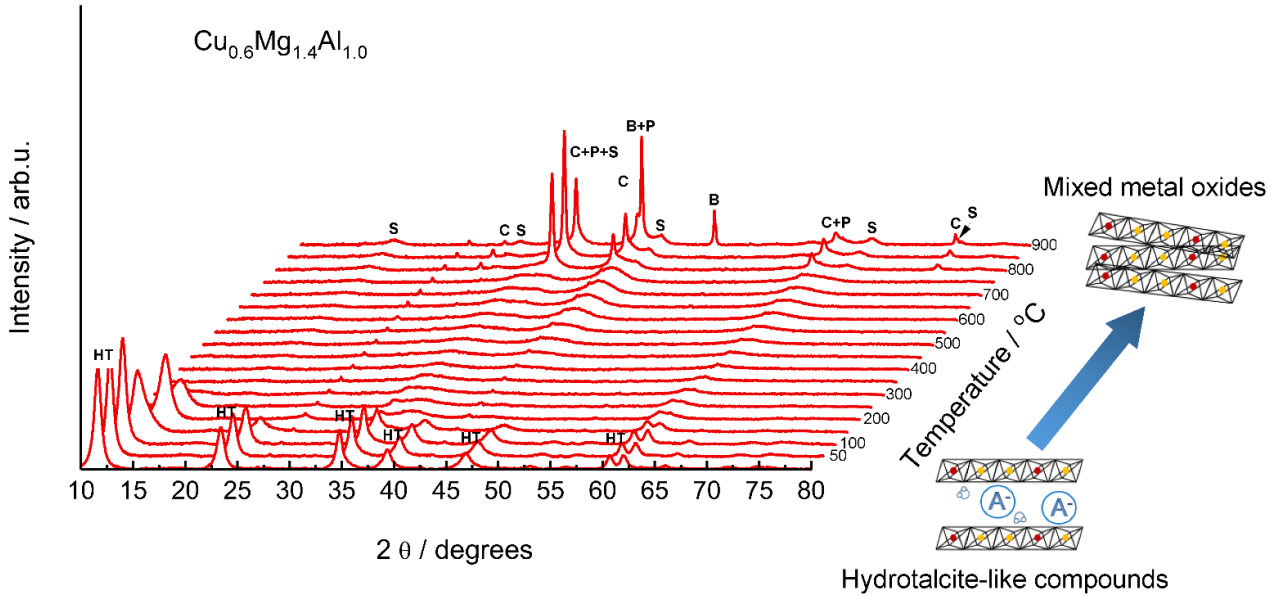

Figure 2. In situ XRD diffraction patterns of the Cu-Mg-Al hydrotalcite-like material recorded in oxidizing conditions. HT—hydrotalcite-like compounds, P—MgO (periclase), C—Cu_2O (cuprite), S—$MgAl_2O_4$ (magnesium aluminate) and/or $CuAl_2O_4$ (copper aluminate), B—$CuAlO_2$: Reprinted from [28] with permission from Springer.

Table 1. Products obtained from the preparation of the $CuM(II)M(III)CO_3$ hydrotalcite-like compounds. Reprinted from [25] with permission from Elsevier.

Cations	Cations' Ratio	Compounds Identified
CuAl	1.0/1.0	Amorphous species
CuZnAl	2.0/1.0/1.0	HT + R
CuZnAl	3.3/1.6/1.0	HT + R
CuZnAl	1.6/0.8/1.0	HT + R
CuZnAl	1.5/1.5/1.0	HT (HT + R)
CuZnAl	1.2/1.2/1.0	HT
CuZnAl	0.8/0.8/1.0	HT
CuCr	1.0/1.0	Amorphous species
CuZnCr	1.5/1.5/1.0	HT
CuCoCr	2.0/2.0/1.0	HT + M
CuCoCr	1.5/1.5/1.0	HT
CuZnCr	1.5/1.5/1.0	HT
CuMgCr	1.5/1.5/1.0	HT
CuMnCr	1.5/1.5/1.0	$MnCO_3$ + HT
CuCoZnCr	1.4/0.1/1.5/1.0	HT
CuZnAlCr	3.0/3.0/1.0/1.0	HT
CuZnFe	1.5/1.5/1.0	Au

HT—hydrotalcite-like compounds; M—$Cu_2CO_3(OH)_2$ (malachite); R—$(Cu,Zn)_2CO_3(OH)_2$ (Rosasite); Au—aurichalcite.

The hydrotalcite-like compounds are used as the precursors for the catalysts more often than as layered materials themselves. During the thermal treatment, the HT-like compounds transform first to an amorphous oxide and then, at higher temperatures, to crystalline mixed metal oxides (Figure 2). The hydrotalcite-derived mixed metal oxides are characterized by key features such as relatively high specific surface area, homogenous dispersion of active metal ions, non-stoichiometry, and high thermal stability, etc. [15].

To the best of our knowledge, Trombetta et al. [29] reported for the first time the catalytic activity and N_2 selectivity over the CuMgAl hydrotalcite-derived mixed metal oxides in NH_3-SCO in 1997. They tested CuMgAl with n(Cu)/n(Mg)/n(Al) of 4.6–7.2/63.8–66.4/29 and found nearly full NH_3 conversion at ca. 400–500 °C and N_2 selectivity below 80%. Following such studies, Chmielarz et al. [30] studied the activity of hydrotalcite-derived mixed metal oxides (M(II, III)Mg(II)Al(III)) containing Ni, Fe, Cu or Co, and pointed out that both the kind and the number of metal ions introduced into hydrotalcite-like structure influenced the activity and selectivity in NH_3-SCO. Among the investigated compositions, Cu-containing catalysts (CuMgAl; n(Cu)/n(Mg)/n(Al) = 5/66/29, 10/61/29, 20/51/29) were the most active in NH_3-SCO, while the Fe-containing one (FeMgAl; n(Fe)/n(Mg)/n(Al) = 10/61/29) revealed enhanced N_2 selectivity. Based on these results, the catalytic properties were further optimized by the combination of both metals, i.e., the introduction of copper and iron ions into the brucite-like structure. The CuMgFe mixed metal oxides with different compositions, such as n(Cu)/n(Mg)/n(Fe) = 0–1/2/1, mol.% (with the optimum composition guaranteeing enhanced NH_3 conversion and N_2 selectivity being n(Cu)/n(Mg)/n(Fe) = 0.5/2/1 [31]) or n(Cu)/n(Mg)/n(Fe) = 5–15/52–62/33 (with the optimum composition of n(Cu)/n(Mg)/n(Fe) = 12/55/33 [32]) were reported. The temperature-programmed studies, i.e., sorption of NH_3 and desorption in He or O_2/He, as well as NH_3-SCR-DeNO$_x$ and NH_3-SCO with different spaces velocities, revealed that the reaction over the CuMgFe hydrotalcite-derived mixed metal oxides proceeds according to the i-SCR mechanism and NH_3 oxidation to NO is a rate-determining step (Figure 3) [31]. Thus, the modification of hydrotalcite-derived materials with noble metals (Pt, Pd, Rh) arose based on those studies [33].

Copper loading at about 5–8 mol.% in the CuMgAl mixed metal oxides allowed reaching full NH_3 conversion at 375–600 °C with N_2 selectivity above 60% [34]. The increase in copper loading led to the formation of bulk-like copper oxide species. The N_2 selectivity varied depending on the catalysts' composition and the method used for the preparation of the hydrotalcite-like precursor. CuMgAl mixed metal oxides prepared via coprecipitation (cop.), and subsequent calcination of the hydrotalcite-like precursor revealed a significantly higher activity and N_2 selectivity compared to the material with similar composition obtained via rehydration (reh.) of calcined Mg-Al hydrotalcite-like compounds or thermal decomposition (decom.) of nitrate precursors (Figure 4a). This effect was ascribed to the presence of the highly dispersed copper oxide species in hydrotalcite-derived mixed metal oxides. Additionally, the catalysts containing the same copper content, but with variations in the n(Mg)/n(Al) ratio presented similar catalytic activity [34,35]. Beyond the optimization of the kind and loading of metal species, the optimization of the calcination temperature is also relevant. The thermal treatment of hydrotalcite-like materials influences the composition of mixed metal oxides and their physico-chemical properties and thus, the activity and N_2 selectivity in NH_3-SCO [28,35]. Hydrotalcite-derived CuMgAl, CuZnAl, CuMgFe mixed metal oxides calcined at 900 °C revealed significantly lower activity compared to the materials calcined at 600 °C (Table 2, pos. 5, Figure 4b), which was ascribed to the different copper oxide phases and their redox properties. Enhanced activity at low temperatures together with a drop of N_2 selectivity at higher temperatures were driven by the easily reduced copper oxides species. Otherwise, calcination temperature at ca. 800 °C led to the formation of the spinel phases, e.g., $Cu_{1-x}Mg_xAl_2O_4$ of lower reducibility, which caused higher N_2 selectivity [35].

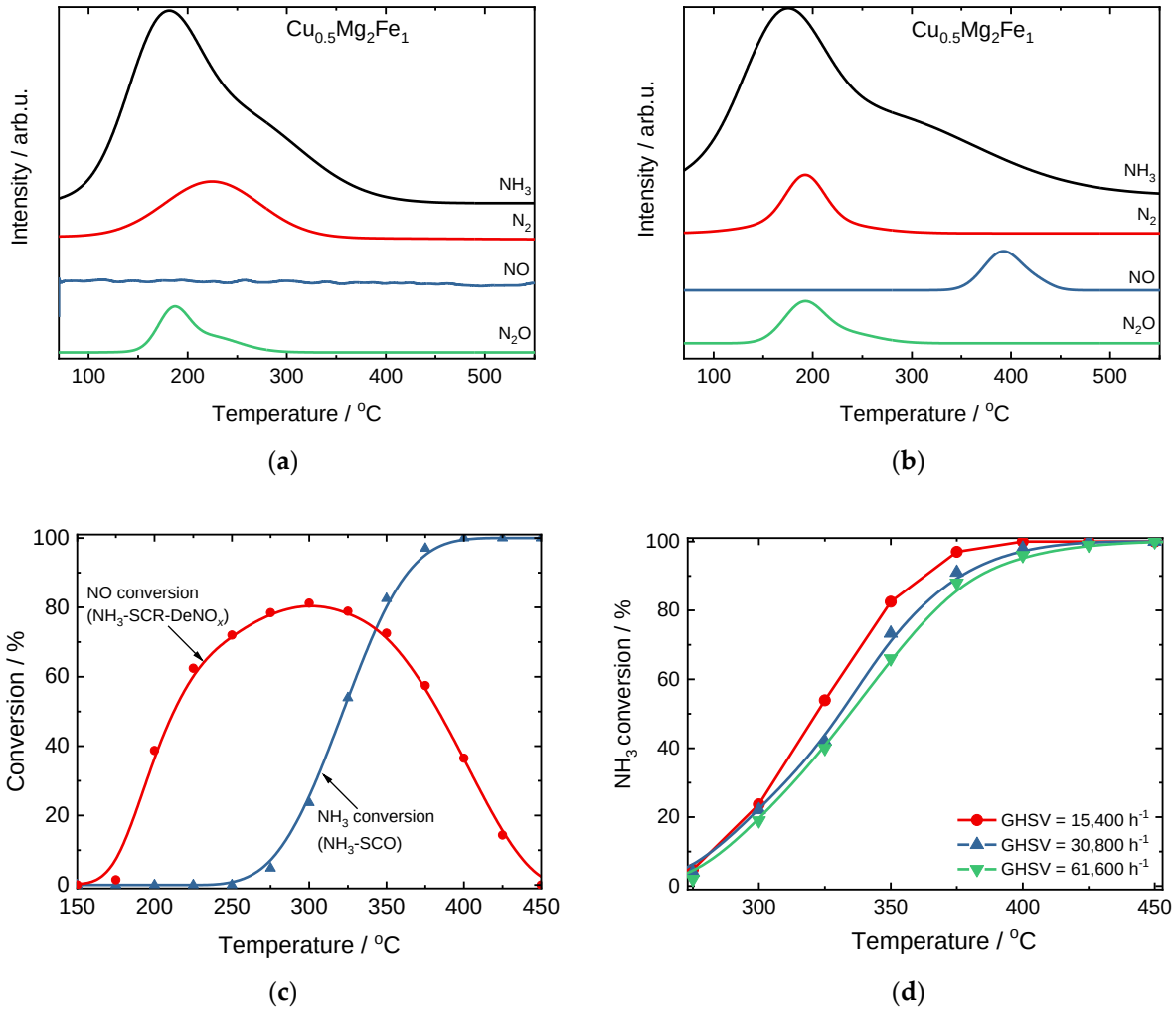

Figure 3. Results of temperature-programmed desorption of NH_3 in (**a**) pure He or (**b**) 5 vol.% O_2/He, adsorption: 70 °C, 1 vol.% NH_3/He, (**c**) comparison of conversion of NH_3 and NO, and (**d**) comparison of the space velocities (SV) over the CuFeAl hydrotalcite-derived mixed metal oxides. Reprinted from [31] with permission of Springer.

Regarding the use of other metals as dopants in Cu-containing mixed metal oxides, Jabłońska et al. [36] introduced Ag, Ce and Ga (y = 0–1 mol.%) to the CuMgAl mixed metal oxides (n(M)/n(Cu)/n(Mg)/n(Al) = y/5/66-y/29). The redox properties determined the catalytic properties for materials with the loading of $y \leq 0.25$, while for the higher metal loading ($y \geq 0.25$) the catalytic properties were driven mainly by the metal oxide phases. Górecka et al. [37] investigated hydrotalcite-derived (5 mol.%) CuMgAl mixed metal oxides, also impregnated with cerium (4 wt.%) over different feed compositions, i.e., NH_3 and O_2 (2 vol.% *versus* 20 vol.%). Higher O_2 concentration enhanced NH_3 conversion, while N_2 selectivity dropped (the opposite effect was found for higher NH_3 concentration in the feed). The effect of the enhanced NH_3 activity over Cu-doped samples was ascribed to the synergetic effect of Ce-Cu redox pairs, which activated the lattice oxygen to react with NH_x species towards the formation of N_2 (Equation (5)). The oxygen vacancies were filled again with the surface oxygen as the cerium and copper species were oxidized (Equation (6), where □ represents oxygen vacancies):

$$Ce^{4+} - O^{2-} - Cu^{2+} + NH_x \rightarrow Ce^{3+} - \square - Cu^{+} + N_2 + H_2O \quad (5)$$

$$Ce^{3+} - \square - Cu^{+} + O_2 \rightarrow Ce^{4+} - O_2 \text{ - } Cu^{2+} \quad (6)$$

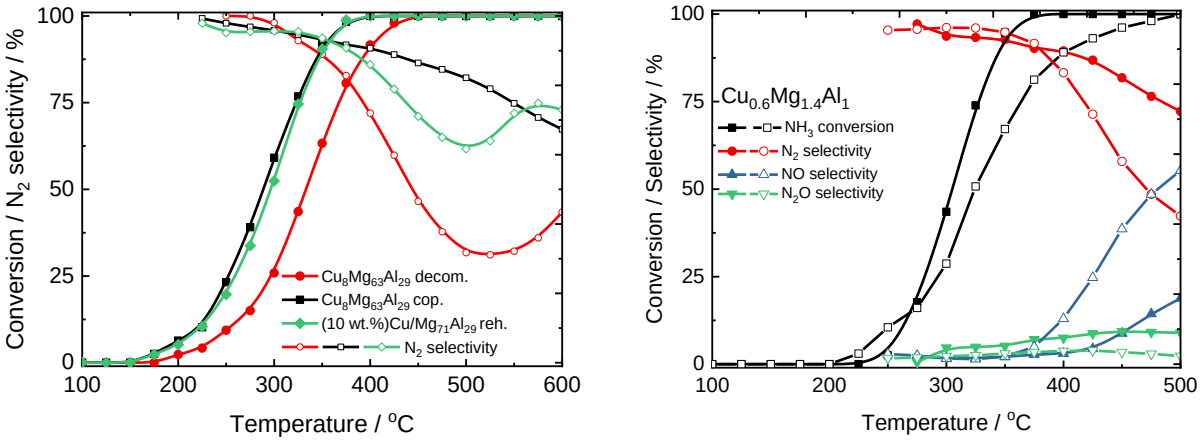

Figure 4. (**a**) Results of NH_3-SCO over the CuMgAl mixed metal oxides. Reprinted from [34] with permission from Elsevier, and (**b**) results of NH_3-SCO over the hydrotalcite-derived mixed metal oxides calcined at 600 and 900 °C. Reprinted from [28] with permission from Springer.

However, from such studies, it was not clear why a rather high Ce loading was applied, since previous research showed that lower cerium loading (0.5 wt.% *versus* 3 wt.%) led to improved catalyst activity in NH_3-SCO [38]. Nevertheless, even higher Ce loading (8.14 wt.%) was applied in further studies over the hydrotalcite-derived CuZnAl mixed metal oxides [39]. Overall, such systems revealed significantly lower N_2 selectivity compared to the Ce/CuMgAl mixed metal oxides (Table 2, pos. 10). N_2O was a minor by-product. Nevertheless, it is also worth mentioning that the Co-Mn-containing materials were reported to selectively oxidize NH_3 to N_2O (ca. 100% below 250 °C) [40].

Concluding, the above-mentioned examples show that the hydrotalcite-derived mixed metal oxides offer a large variety of possible modifications and tuning of their properties, which makes them suitable for NH_3-SCO applications. Mainly Cu-containing hydrotalcite-derived mixed metal oxides were applied for NH_3 oxidation to N_2. Overall, the full NH_3 conversion between 375–650 °C and N_2 selectivity above 70% (based on the data gathered in Table 2, depending on the catalyst composition and preparation, reaction conditions, etc.), were achieved over the Cu-containing hydrotalcite-derived mixed metal oxides. Thus, further optimization of both chemical and phase compositions could lead to enhanced NH_3 conversion and N_2 selectivity below 350 °C. Still, intensive studies focused on the development of such catalytic systems in NH_3-SCO are required under application-relevant reaction conditions (i.e., minor NH_3 slip (O_2 excess), up to 600–700 °C (in the cycle of diesel particulate filter regeneration) in the presence of H_2O, CO_x and/or SO_x), including an investigation of the reaction mechanisms.

3. Other Metal Oxides

In the literature, various types of other metal oxides (still excluding noble metal-doped catalysts and zeolite-based materials) have been reported for NH_3-SCO. The investigation of Co_3O_4, MnO_2, CuO, Fe_2O_3 and V_2O_5 in NH_3-SCO was reported in the early studies of Il'chenko and Golodets in 1975 [41,42]. The specific catalytic activities at 230 °C ($p(NH_3)$ = 0.1 atm, $p(O_2)$ = 0.9 atm) of the selected metal oxides decreased in the following sequence: Co_3O_4, MnO_2 > CuO > NiO > Bi_2O_3 > Fe_2O_3 > V_2O_5 > TiO_2 > ZnO > WO_3. Among the transition metals, V_2O_5, MoO_3 and WO_3 exhibited nearly 100% N_2 selectivity at 230 °C [43]. A similar activity order (MnO_2 > Co_3O_4 > CuO > Fe_2O_3 ≈ V_2O_5 > NiO) was found by Hinokuma et al. [44] under 1 vol.% NH_3, 0.75 vol.% O_2, He balance. CuO reached higher N_2 selectivity than other oxides [43,45].

NH_3-SCO (as a side process) has been frequently studied with NH_3-SCR-DeNO_x, thus, the following studies focused on the supported V-containing catalysts, e.g., V_2O_5/TiO_2 [46,47]

V_2O_5/TiO_2-SiO_2 [48], V_2O_5-WO_3/TiO_2 [46,49], V_2O_5-WO_3/ZrO_2 [50], etc. E.g., Ueshima et al. [51] examined different supports for V_2O_5-WO_3 and found the decreasing order of catalytic activity in terms of support as follows: TiO_2-SiO_2 (binary oxide) > TiO_2 (anatase) > TiO_2 (rutile) > SiO_2. Contrary to such studies, V_2O_5 supported on the rutile form of TiO_2 led to a more active and N_2 selective (below 400 °C) catalyst [47]. In another study, V_2O_5/MgO was the least active among vanadium oxide supported on TiO_2, SiO_2 or MgO [52]. Furthermore, the commercial V_2O_5-WO_3-TiO_2 catalyst was modified with Cu (1 wt.%) and Ce (1–10 wt.%) species. Overall, the catalyst with the composition of (1.02 wt.%)Cu-(4.79 wt.%)Ce/V_2O_5-WO_3-TiO_2 showed enhanced activity at 300 °C, while its modification with Ce enhanced H_2O and sulfur resistance [53]. The V_2O_5-WO_3-TiO_2 catalyst modified with Cu or Fe (1.0 wt.%) ions revealed the highest activity and N_2 selectivity above 350 °C (among other materials modified with Mn or Co species) [54]. Furthermore, K_2O was also suggested (but not experimentally tested) as an effective promoter for the V_2O_5/TiO_2 and V_2O_5-WO_3/TiO_2 catalysts for NH_3-SCO at 500 °C. Regarding, the reaction mechanisms in NH_3-SCO, Yuan et al. [55] performed density functional theory (DFT) calculations in conjunction with cluster models on the V_2O_5 surfaces. According to such mechanisms (Figure 5a), NH_3^+ appears as the initial intermediate from the activated NH_3 which transfers an electron to the metal oxide surfaces. Further routes, depending on the availability of the O_2 species, can arise, i.e., the *direct route* appears in the case of limited O_2 or its absence. Consequently, formed N_2H_4 was oxidized to N_2 on V=O sites. In the presence of O_2, $NH_3O_2^+$ complex was formed, which further decomposes to NO (followed by NH_3-SCR-DeNO$_x$) with the N_2 formation. Such an *indirect route* (i.e., i-SCR mechanism) was reported also over the V-based catalysts [53,54] (e.g., Figure 5b). Recently, Liu et al. [56] identified based on the first-principle calculation method of DFT the adsorption sites of NH_3 on V_2O_5(001).

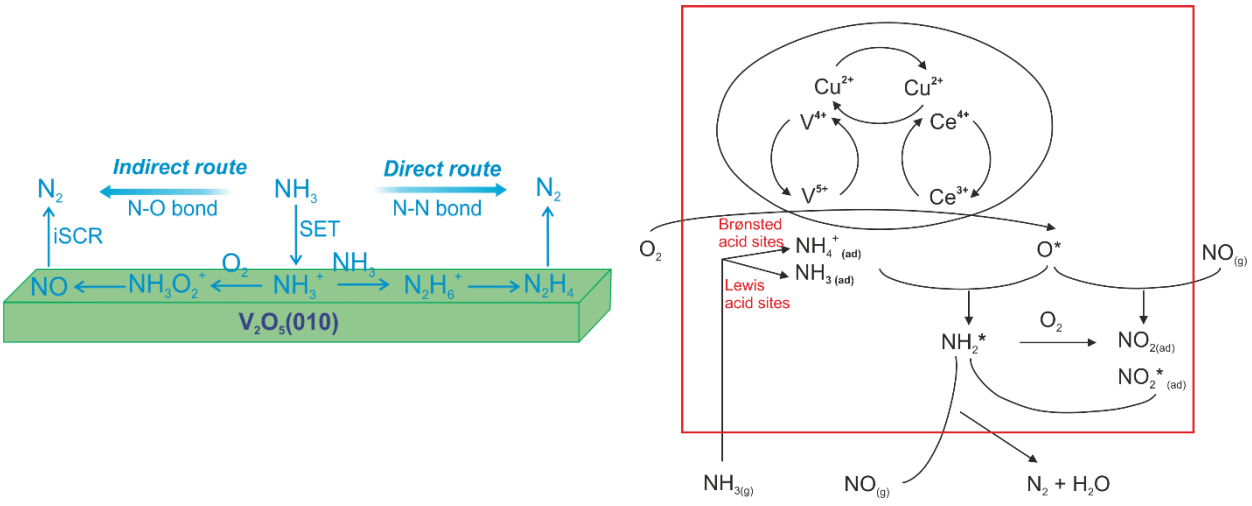

Figure 5. (**a**) Two competitive routes for NH_3 oxidation over V_2O_5(010). Reprinted from [55] with permission from ACS Publications; (**b**) schematic representation of the mechanism of NH_3-SCO over Cu-Ce/V_2O_5-WO_3-TiO_2. Reprinted from [53] with permission from Elsevier.

Carley et al. [57] revealed the structural characteristics of imide strings formed when a Cu(110) surface was exposed to the NH_3-O_2 mixture (30 vol.%–1 vol.%, 52 °C, 10^{-8} mbar —UHV investigations). Contrary to that, no imide species were found on the surface of polycrystalline copper in NH_3-SCO at 1.2 mbar [58]. CuO was found to selectively oxidize NH_3 to N_2O, while Cu_2O to N_2, respectively [58,59]. Hirabayashi and Ichihashi [60] investigated reactions of copper oxide cluster cations, $Cu_nO_m^+$ (n = 3–7, $m \leq 5$) with NH_3 at near thermal energies using a guided ion beam tandem mass spectrometer. Depending on the applied clusters, H_2O, O_2 or -HNO were released, while the release of N_2 was observed in the multiple-collision reactions of $Cu_5O_3^+$ and $Cu_7O_4^+$ clusters. Never-

theless, it is recognized that supported copper species (e.g., Cu/Al_2O_3 [61,62], CuO/carbon nanotubes [63]) or the combination of CuO and other transition or rare earth metal oxides, e.g., Fe_2O_3, CeO_2, La_2O_3, $CuCr_2O_4$ and $CuCrO_2$ or $La_2Ce_2O_7$ (nonporous pyrochlore structure—$A_2B_2O_7$) (e.g., [61,62,64–67]) result in catalysts with enhanced activity and N_2 selectivity in NH_3-SCO. E.g., Gang et al. [61,62] and afterward other authors [68–71] have proved the high catalytic activity of copper species deposited on γ-Al_2O_3. They claimed that copper species dispersion becomes poorer on Al_2O_3 at metal loading higher than ca. 10 wt.% (among 5–15 wt.%) [62]. Furthermore, many studies about similar catalytic systems concur on ca. 10 wt.% as an optimum loading of copper species [4]. The full NH_3 conversion of this group appears at 350–500 °C with N_2 selectivity above 75% (Table 2) depending on the preparation methods (e.g., copper precursors [70,72], treatment strategies [9]), and reaction conditions (e.g., fuel-lean/rich conditions [71,73,74]). Based on the studies of Lenihan and Curtin [69], the stability of Cu/Al_2O_3 through the dry, wet and subsequently dry conditions was proved. Moreover, the activity of CuO/Al_2O_3 catalyst was further enhanced by its dopping with PbO, NiO, CoO or SnO (with $\leq$ 1 wt.% loading of dopant) [68]. Not only has γ-Al_2O_3 been applied as the catalyst support, η-Al_2O_3 has also been employed [75]. Still, the full NH_3 conversion appeared around 550 °C over (1–2 wt.%)Cu/η-Al_2O_3. The catalytic properties of Cu/Al_2O_3 were further increased via its modification with Li_2O and CeO_x. Above 250 °C the materials were only N_2 selective [76]. In addition, increasing the $c(O_2)/c(NH_3)$ ratio enhanced the conversion. Recently, Machida et al. [77] investigated several nanometer-thick transition metal (mainly noble metals but also Cu or Co) overlayers formed on a Fe-Cr-Al metal (SUS) foil by pulsed cathodic arc-plasma deposition. The activity of the Co- and Cu-based materials decreased significantly in the presence of 10 vol.% H_2O (while those of the catalysts containing Pt and Ir remained nearly unchanged, i.e., preserved the active metallic surface during NH_3-SCO in the presence of O_2/H_2O).

Other than Cu, other metal species such as Ni, Mn, Fe, Co, Mg and Zn were supported on Al_2O_3 [78]. For the (10 wt.%)Ni-containing catalysts, the activity was found to decrease in the order of γ-Al_2O_3, ZrO_2, MgO > SiO_2 > TiO_2 >ZSM-5, with full NH_3 conversion being reached at 550 °C for Ni/Al_2O_3 (possibly due to presence of $NiAl_2O_4$). The catalytic properties of the samples loaded above 10 wt.% tend to become similar to that expected for pure NiO. Furthermore, Mn/Al_2O_3 and Fe/Al_2O_3 were proved to be more active (full NH_3 conversion at 300–500 °C with N_2 selectivity > 70%) than Ni/Al_2O_3 (550 °C) for NH_3 oxidation, possibly because of their enhanced redox properties. In addition, several groups have investigated Ni-based catalysts above 500 °C (e.g., prepared via microemulsion) [79,80].

He et al. [65] demonstrated that TiO_2 is a more suitable support (due to the higher oxygen mobility and lower oxygen bonding strength) than Al_2O_3 for copper-based catalysts, which was represented by the enhanced catalytic properties of Cu/TiO_2 compared to Cu/Al_2O_3. Contrary to that, for the Cu-Mn species, deposition on Al_2O_3 (compared to TiO_2) guaranteed enhanced activity [81]. In the case of Cu/TiO_2, NH_3 conversion was reported to depend on the Cu species loading, e.g., for (10 wt.%)Cu/TiO_2 full conversion occurs at about 250 °C with 95% N_2 selectivity [65], while for (1 wt.%)Cu/TiO_2—425–500 °C with < 60% N_2 selectivity was reported [82]. Duan et al. [83] investigated (10 wt.%) V, Cr, Zn and Mo supported on TiO_2. Comparatively tested Cu/TiO_2 and Cr/TiO_2 revealed lower NO and NO_2 selectivity over chromium-containing catalysts. The applied O_2 content in the feed gas ranging from 0.5 vol.% to 5 vol.% revealed similar NH_3 conversion (with an exception below 150 °C where NH_3 conversion was higher in the presence of 0.5 vol.% O_2). Moreover, NO selectivity was not affected by the different O_2 content during NH_3-SCO. TiO_2 anatase is the most common catalyst support, while the catalytic properties are affected by the properties of the support (i.e., anatase *versus* rutile) [84]. NH_3-SCO over $Cu/TiSnO_2$ and Cu/TiO_2 (10.5–11.8 wt.% of Cu) was reported to follow the i-SCR and imide (-NH) mechanisms, respectively [85]. For the i-SCR mechanism (Figure 6), NH_3 was first adsorbed on both Lewis and Brønsted acid sites. After that, it reacted with surface-active oxygen

species to form nitrate species (intermediates in NH_3-SCO), which finally reacted with the remaining NH_3 with the formation of N_2 and H_2O. Gaseous NH_3 recombined with the released acid sites to participate in the next cycles.

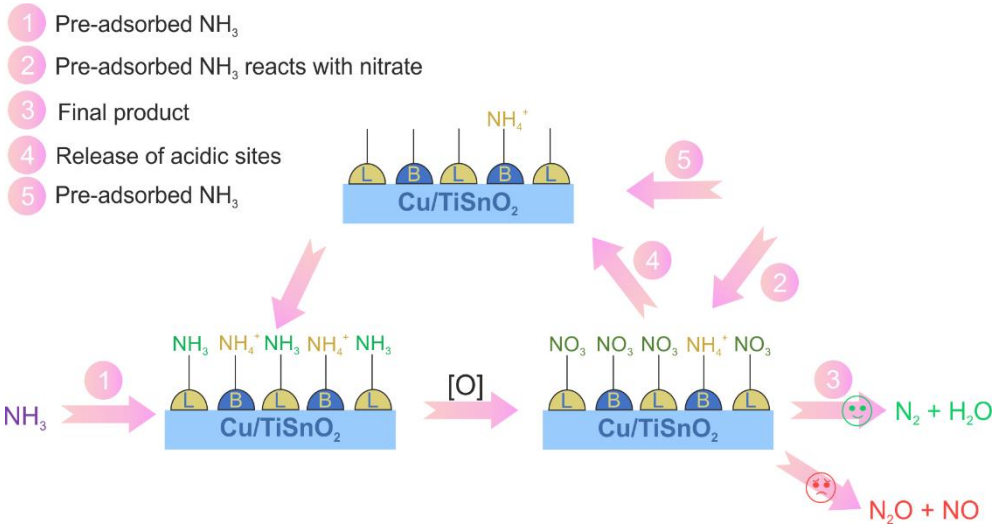

Figure 6. Reaction mechanism of NH_3-SCO over $Cu/TiSnO_2$. Reprinted from [85] with permission of Elsevier.

The bands assigned to nitrate species were also found using in situ DRIFTS in the spectra of a series of CuO-Fe_2O_3 catalysts (with an optimum at n(Cu):n(Fe) molar ratio of 5:5 with full NH_3 conversion > 250 °C) recorded at 250 and 350 °C [86]. The authors proposed the molecular steps of the i-SCR mechanism, in which the nitrosyl (-HNO) species were formed via a reaction between adsorbed NH_{3-x} species with atomic oxygen (Equations (7)–(10)). Then, the -HNO was oxidized by oxygen atoms from O_2 to form NO species (Equations (11) and (12)). Additionally, the -NH species interacted with O_2 to form NO. Meanwhile, the in situ-formed NO could react with -NH_x to form N_2 or N_2O (Equations (13) and (14)).

$$NH_3 \rightarrow NH_2 + H \quad (7)$$

$$NH_2 \rightarrow NH + H \quad (8)$$

$$NH + O \rightarrow HNO \quad (9)$$

$$O_2 \rightarrow 2O \quad (10)$$

$$HNO + O \rightarrow NO + OH \quad (11)$$

$$NH + O_2 \rightarrow NO + OH \quad (12)$$

$$NH_2 + NO \rightarrow N_2 + H_2O \quad (13)$$

$$NH + NO \rightarrow N_2O + H \quad (14)$$

$$H + OH \rightarrow H_2O \quad (15)$$

To reveal the impact of calcination temperature on the catalytic properties of the CuO-Fe_2O_3 catalysts (at n(Cu)/n(Fe) molar ratio of 1/1), the materials were calcined between 400 and 700 °C [87]. Among them, CuO-Fe_2O_3 calcined at 500 °C revealed full NH_3 conversion at ca. 225 °C, i.e., at about 25 °C lower than for the material calcined at 400 °C. The increase in the calcination temperature (up to 600–700 °C) resulted in a decrease in the activity in NH_3-SCO, while selectivity was not affected. The simultaneous addition of H_2O and SO_2 to the feed gas led to a drop in activity and N_2 selectivity. Regarding the application of the Cu-Fe-containing spinel, Yue et al. [88] found that for

the mesoporous $CuFe_2O_4$—prepared with KIT-6 as the hard template, NH_3 was nearly completely consumed at 300 °C while the N_2 selectivity dropped below 90% up to 600 °C. $CuMoO_4$, $CoMoO_4$ or $FeMoO_4$ were significantly less active in NH_3-SCO [45]. For $CuMoO_4$, activity and N_2 selectivity were completely inhibited by water vapor (10 vol.%). Beyond fully synthesized materials, natural vermiculite and phlogopite [89–91] or attapulgite [92] modified with Cu or Fe species are also active and N_2 selective catalysts for NH_3-SCO (Table 2, pos. 42–46).

Similar to pure CuO and NiO, for CeO_2 the catalytic activity was also poor [93,94]. Despite this, the (10 wt.%)Ce/TiO_2 catalyst (calcined at 400–500 °C) revealed enhanced activity in NH_3-SCO between 300–350 °C but did not reach full NH_3 conversion [94]. Furthermore, the catalytic activity increased from 50 to 90% at 300 °C for (10 wt.%)Ce/TiO_2 after its modification with vanadium (2 wt.%) [95]. This effect was assigned to the dispersion of Ce^{4+} species on TiO_2. The $V/Ce/V/TiO_2$ catalyst showed resistance to SO_2 poisoning due to the reduced formation of the NH_4HSO_4 species. The Ce-containing mixed metal oxides constitute a representative group of catalysts for NH_3-SCO. E.g., Wang et al. [93] investigated a series of $Ce_{1-x}Zr_xO_2$ ($0.2 \leq x \leq 0.8$) mixed oxide catalysts, among which particularly $Ce_{0.4}Zr_{0.6}O_2$ reached the total NH_3 oxidation of about 360 °C (N_2 selectivity > 90%). $Ce_{0.4}Zr_{0.6}O_2$ was also subjected to further modifications with Ru species [96]. Cu-Ce-Zr catalyst prepared by a citric acid sol-gel method exhibited the highest activity among other materials (prepared via the homogenous precipitation and incipient wetness impregnation methods) achieving full NH_3 conversion at 230 °C with > 90% N_2 selectivity [97]. These results were attributed to the finely dispersed CuO, the Cu-Ce-Zr solid solution and the monomeric Cu^{2+} ions in octahedral sites (in contrast to monomeric Cu^{2+} in the square-planar pyramidal sites). Moreover, the adsorbed oxygen species were more active than the bulk lattice oxygen species in NH_3-SCO. The co-presence of SO_2 and H_2O or CO_2 in the feed resulted in the NH_3 conversion decreasing to 92 and 81%, respectively. NH_3-SCO over the catalysts prepared via different techniques followed the i-SCR mechanism (with the -NH_x and -HNO intermediates, Figure 7a) [98].

Lou et al. [99] have reported nearly complete NH_3 conversion at temperatures as high as 400 °C with an overall N_2 selectivity varying from 19 to 82% over Cu-Ce mixed oxides prepared by coprecipitation with an optimum at $n(Cu)/n(Ce) = 6/4$ (among 6–9/1–4). Afterward, the $CuO\text{-}CeO_2$ catalysts prepared by a surfactant-templated method exhibited full NH_3 conversion below 300 °C with more than 90% N_2 selectivity [100]. However, the thermal resistance of $CuO\text{-}CeO_2$ mixed oxides needs to be further enhanced. The finely dispersed CuO species as well as a strong synergetic interaction between the copper oxide species and cerium oxides significantly decreased the operation temperature. Thus, activated ammonia reacted with lattice oxygen in the Cu-O-Ce solid solution generating N_2 and H_2O, while gaseous O_2 regenerated the oxygen vacancies in the Cu-O-Ce solid solution to maintain Ce^{4+}/Ce^{3+} redox couple (Figure 7b). NH_3 was oxidized over CeO_2 to NO, which in the next step reacted with NH_x forming N_2 over CuO (according to the i-SCR mechanism). CuO/La_2O_3 ($n(Cu)/n(La)$ = 6–9/1–4 with an optimum at 8/2) showed a significantly lower activity and N_2 selectivity of 93 and 53% at 400 °C, respectively [64], compared to $CuO\text{-}CeO_2$ (e.g., 98–99% NH_3 conversion with 85–86% N_2 selectivity at 400 °C for $n(Cu)/n(Ce) = 6/4$) [101,102].

Mn-based catalysts have been demonstrated to be active in NH_3-SCO. E.g., natural manganese ore (NMO, consisting of manganese oxides and small amounts of Fe_2O_3, CaO, MgO, SiO_2, Al_2O_3) was recognized as a low-cost catalyst possessing similar activity (ca. 50 % NH_3 conversion) to that of MnO_2 below 150 °C. Above 150 °C, Mn_2O_3 was the most active one. Across the studied temperatures between 50–250 °C, N_2 selectivity decreased as follows: NMO > MnO_2 > Mn_2O_3 [103]. Mn_2O_3 supported on TiO_2 (anatase containing 1.15 wt.% sulfate) revealed significantly lower activity at 277–307 °C than the supported Cu-Mn mixed oxides ($n(Cu)/n(Mn)$ = 20–80/20–80) [104]. It was found that the most active catalyst (with $n(Cu)/n(Mn) = 20/80$) contained a $Cu_{1+x}Mn_{2-x}O_4$ crystalline spinel phase and X-ray amorphous Mn^{2+}-containing species. Unfortunately, the selectivity

was not reported. The activity of Cu-Mn/TiO_2 was further enhanced via its modification with Ce or La species [105]. Ce-Cu-Mn/TiO_2 prepared through the sol-gel method was the most active among the catalysts prepared via impregnation or coprecipitation and reached complete NH_3 conversion at ca. 200 °C, however with 96% NO selectivity. Song et al. [106] investigated a series of MnO_x(*z*)-TiO_2 [106] (*z* = 0.1–0.3) prepared by the sol-gel method. The optimum MnO_x(0.25)-TiO_2 showed nearly full NH_3 conversion around 200 °C with N_2 selectivity of more than 60% up to 350 °C. NO was formed only above 250 °C. Based on the in situ DRIFTS studies, they claimed that N_2 appeared as a product of the reaction between -HNO and -NH species. N_2O was formed from the combination of two -HNO species at low temperatures, as well as from the reaction between adsorbed NH_3 and nitrite/nitrate species at high temperatures. Additionally, the i-SCR mechanism was proposed over Fe_2O_3-Al_2O_3, Fe_2O_3-TiO_2, Fe_2O_3-ZrO_2 and Fe_2O_3-SiO_2 prepared by the sol-gel method [107]. The materials prepared from iron sulfate led to a higher N_2 selectivity than those prepared from nitrate. The higher N_2 selectivity was reported earlier for CuO/TiO_2 prepared from $CuSO_4$ compared to the corresponding catalyst prepared from $Cu(NO_3)_2$ [52], which is also valid for the pre-sulfated samples [68].

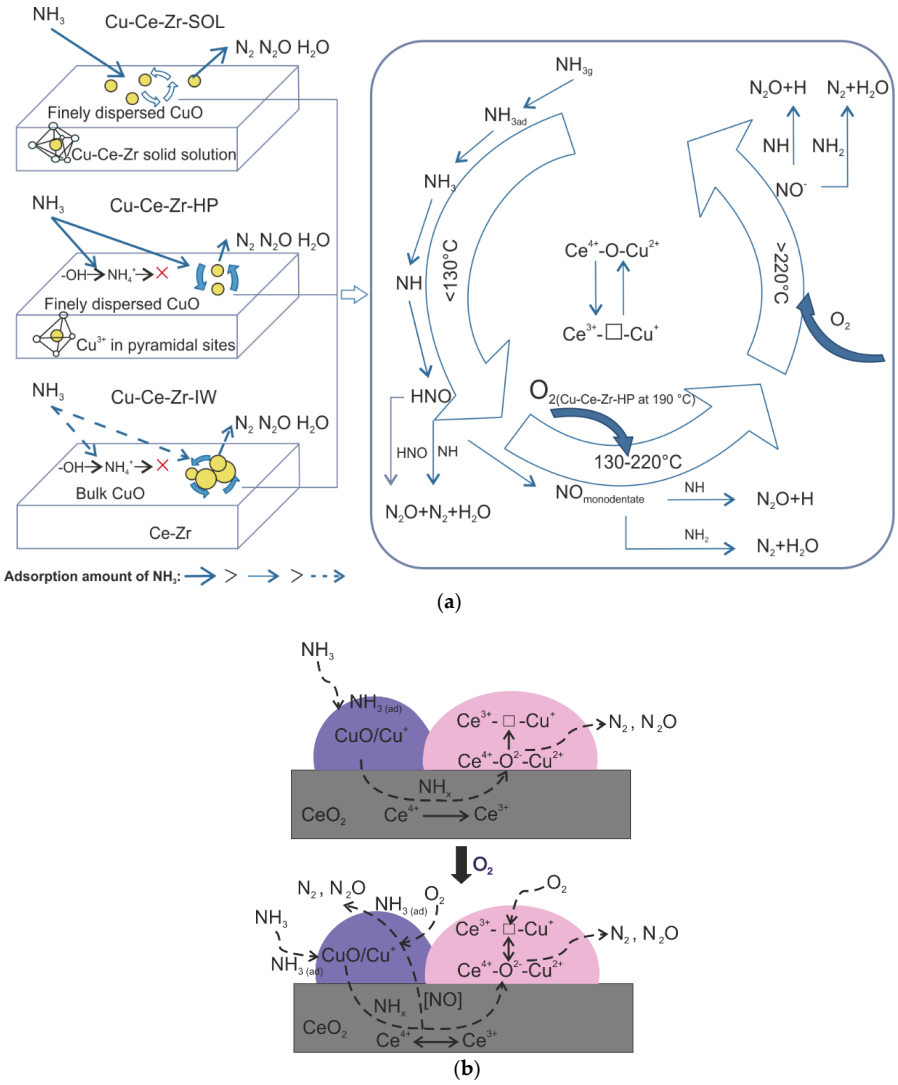

Figure 7. (**a**) Relationship of activity-adsorption-structure and reaction pathway over Cu-Ce-Zr prepared via different synthesis routes; SOL—citric acid sol-gel method; HP—homogeneous precipitation, IW— incipient wetness impregnation. Reprinted from [98] with permission from Elsevier; (**b**) NH_3-SCO oxidation over CuO-CeO_2. Reprinted from [100] with permission from Elsevier.

Chen et al. [108] developed a series of mullite-based AMn_2O_5 (A = Sm, Y, Gd) catalysts, among which $SmMn_2O_5$ achieved complete NH_3 conversion at 175–250 °C (albeit with a rather low N_2 selectivity of barely more than 45%). The imide mechanism was reported for NH_3-SCO over $SmMn_2O_5$. Furthermore, its modification with niobium oxide (5 wt.%)$Nb_2O_5/SmMn_2O_5$ stood out with N_2 selectivity > 60%. The niobium oxide was supposed to enhance the catalyst surface attraction to the N atom lone-pair electron. Consequently, the reaction between the increased amount of -NH and -HNO species towards the formation of N_2 was favored (Figure 8a). In the other approach, $SmMn_2O_5$ was mixed with Cu-SAPO-34 [109]. Still, N_2 selectivity varied between 20–60% in the range of 150–400 °C. For the mixed catalysts, the i-SCR mechanism was proposed (NH_3 oxidation to NO_x over mullite catalyst), which stays contrary to the above-mentioned studies. The i-SCR mechanism was also proposed over the $La_xSr_{1-x}MnO_3$ perovskite-based catalysts post-modified with a 3 M solution of HNO_3 (0.1–72 h, Figure 8b) [110]. As the treatment time increased, the perovskite phase changed from a mixture of perovskite and MnO_2 (10 h treatment) to pure MnO_2 (72 h treatment). Additionally, the materials subjected to a 72 h treatment were the most active, albeit selective to NO and N_2O, as well as poorly resistant to sulfur species.

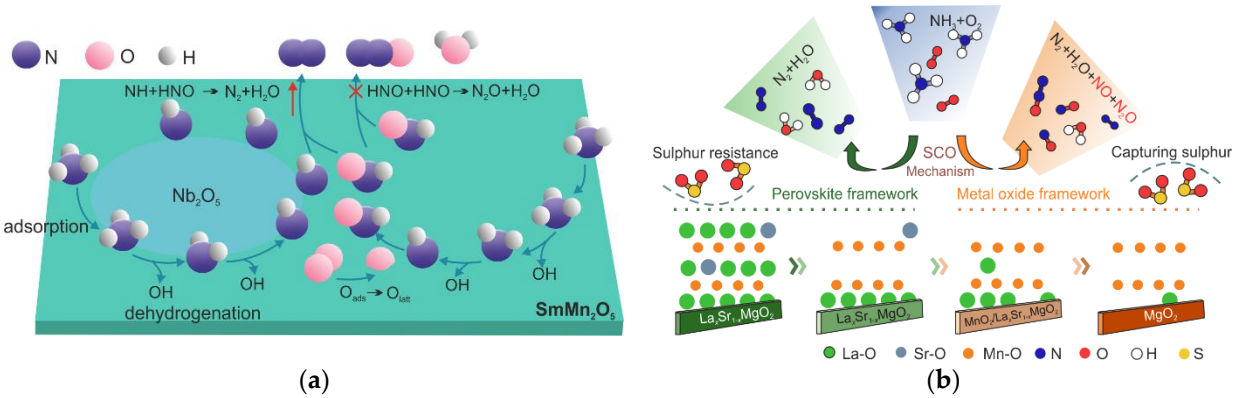

Figure 8. Schematic representation of (**a**) Nb_2O_5 modification to enhance the N_2 selectivity of $SmMn_2O_5$. Reprinted from [108] with permission from Elsevier; (**b**) NH_3-SCO mechanism over modified $La_xSr_{1-x}MnO_3$ perovskite. Reprinted from [110] with permission from ACS Publications.

Concluding, several transition metal-based catalysts were proposed for NH_3 oxidation to N_2. Among them, mainly Cu/Al_2O_3, Cu-Ce-Zr, $CuO-Fe_2O_3$ or $CuO-CeO_2$ were the most frequently studied materials (according to data gathered in Table 2). In the case of Cu/Al_2O_3, the optimal loading of 10 wt.% Cu guarantees an enhanced NH_3 conversion and N_2 selectivity (full NH_3 conversion at 350–500 °C with N_2 selectivity above 75%). For the other mentioned materials, i.e., Fe- or Ce-containing systems, the catalytic studies were carried out only in a narrow temperature range. The complete NH_3 conversion was achieved between 225/250–300 °C with N_2 selectivity above 80% (Table 2). Further attention should be given to the stability under conditions simulating real exhaust from diesel engines up to 600–700 °C of the mesoporous $CuFe_2O_4$ spinel.

Table 2. Comparison of complete NH_3 conversion and N_2 selectivity in the same temperature range over hydrotalcite-derived mixed metal oxides and other transition metal-based catalysts reported in the literature (related data are marked with asterisks).

Pos.	Sample	Preparation	Reaction Conditions	Operation Temperature for Achieving 100% NH_3 Conversion/°C	N_2 Selectivity/%	Refs.
			Hydrotalcite-derived mixed metal oxides			
1	CuMgAl *n*(Cu)/*n*(Mg)/ *n*(Al) = 4.6/66.4/29, mol.%	Coprecipitation, calcination, 650 °C, air, 14 h	0.5 vol.% NH_3, 1.75 vol.% O_2, He balance, GHSV 10,000–12,000 h^{-1}	500	>80	[29]
2	CuMgAl *n*(Cu)/*n*(Mg)/ *n*(Al) = 5/66/29, mol.%	Coprecipitation, calcination, 600 °C, air, 16 h	0.5 vol.% NH_3, 2.5 vol.% O_2, He balance, GHSV 30,000 h^{-1}	400–650	>80	[30]
3	CuMgFe *n*(Cu)/*n*(Mg)/ *n*(Fe) = 0.5/2/1, mol.%	Coprecipitation, calcination, 600 °C, air, 12 h	0.5 vol.% NH_3, 2.5 vol.% O_2, He balance, GHSV 15,400 h^{-1}	400–450	>70	[31]
4	CuMgAl *n*(Cu)/*n*(Mg)/ *n*(Al) = 8/63/29, mol.%	Coprecipitation, calcination, 600 °C, air, 6 h	0.5 vol.% NH_3, 2.5 vol.% O_2, Ar balance, WHSV 24,000 mL h^{-1} g^{-1} * 0.5 vol.% NH_3, 2.5 vol.% O_2, N_2 balance, WHSV 137,000–140,000 mL h^{-1} g^{-1} ** 0.5 vol.% NH_3, 2.5 vol.% O_2, 10 vol.% CO_2, 5 vol.% H_2O, N_2 balance, WHSV 137,000–140,000 mL h^{-1} g^{-1}	400–600 * 450–600 ** 600	>60 * >60 ** >55	[34] *,** [111]
5	CuMgAl *n*(Cu)/*n*(Mg)/ *n*(Al) = 0.6/1.4/1.0, mol.%	Coprecipitation, calcination, 600 °C, *900 °C, air, 12 h	0.5 vol.% NH_3, 2.5 vol.% O_2, He balance, WHSV 24,000 mL h^{-1} g^{-1}	375–500 * 500	>70 * >40	[28]
6	CuMgAl *n*(Cu)/*n*(Mg)/ *n*(Al) = 5/62/33, mol.%	Coprecipitation, calcination, 600 °C, 800 °C *, air, 12 h	0.5 vol.% NH_3, 2.5 vol.% O_2, He balance, WHSV 24,000 mL h^{-1} g^{-1}	475–500 * 475–500	>60 * >85	[35]
7	GaCuMgAl * CeCuMgAl *n*(Ga/Ce)/*n*(Cu)/*n*(Mg)/ *n*(Al) = 0.25/5/65.75/29	Coprecipitation, calcination, 600 °C, air, 6 h	0.5 vol.% NH_3, 2.5 vol.% O_2, Ar balance, WHSV 24,000 mL h^{-1} g^{-1}	375–500 * 375–500	>80 * >50	[36]

Table 2. *Cont.*

Pos.	Sample	Preparation	Reaction Conditions	Operation Temperature for Achieving 100% NH_3 Conversion/°C	N_2 Selectivity/%	Refs.
8	CuMgAl n(Cu)/n(Mg)/n(Al) = 10–15/52–57/33, mol.% * (4.1 wt.%)CeCuMgAl n(Cu)/n(Mg)/n(Al) = 5/62/33, mol.%	Coprecipitation, calcination, 800 °C, air, 9 h * Impregnation, calcination, 800 C, air, 9 h	0.035 vol.% NH_3, 20 vol.% O_2, N_2 balance, WHSV 30,000 mL h^{-1} g^{-1}	350 * 350	<20 * <70	[37]
9	CuMgAl n(Cu)/n(Mg)/n(Al) = 5/62/33, mol.% * (3 wt.%)CeCuMgAl ** (0.5 wt.% Ce)CuMgAl	Coprecipitation, calcination, 600 °C, air, 12 h, *,** Impregnation, calcination, air, 600 °C, 12 h	0.5 vol.% NH_3, 2.5 vol.% O_2, He balance, WHSV 24,000 mL h^{-1} g^{-1}	500–600 * 500–600 ** 450–600	>60 * >75 ** >55	[38]
10	CuZnAl n(Cu)/n(Zn)/n(Al) = 10–15/52/33, mol.% * (8.14 wt.%)CeCuMgAl		0.035 vol.% NH_3, 20 vol.% O_2, N_2 balance, WHSV 30,000 mL h^{-1} g^{-1}	350 * 350	<30 * <40	[39]
11	CoMnAl n(Co)/n(Mn)/n(Al) = 4/1/1	Coprecipitation, calcination, 500 °C, air, 4 h; * Mechanochemical method, calcination, 500 °C, air, 4 h	0.5 vol.% NH_3, 2.5 vol.% O_2, He balance, WHSV 24,000 mL h^{-1} g^{-1}	250–500 * 250–500	>40 * >45	[40]
			Other metal oxides			
12	CuO/monolith	Precursors calcination on the monolith, 600 °C, air, 6 h	0.05 vol.% NH_3, 3 vol.% O_2, N_2 balance, GHSV 40,000 h^{-1}	450–550	67–85	[45]
13	(10 wt.%)V/TiO_2	Impregnation, calcination, 550 °C, air, 6 h	0.05 vol.% NH_3, 2.5 vol.% O_2, N_2 balance, GHSV 35,385 h^{-1}	225–300	-	[83]
14	(10 wt.%)Cu/TiO_2			200–300	-	
15	(10 wt.%)Cu/TiO_2	Impregnation, rotary evaporator, calcination, 450 °C, air, 3 h	0.04 vol.% NH_3, 10 vol.% O_2, He balance, GHSV 50,000 h^{-1} * 0.04 vol.% NH_3, 10 vol.% O_2, 3 vol.% H_2O, He balance, GHSV 50,000 h^{-1}	250–300 * 350–375	>95 * >95	[65]
16	(10 wt.%)Cu/Al_2O_3			400	>95	
17	(10–15 wt.%)Cu/Al_2O_3	Impregnation, calcination, 600 °C, air, 24 h	1.14 vol.% NH_3, 8.21 vol.% O_2, He balance, WHSV 2 240 mL h^{-1} g^{-1}	350	>90	[61]

Table 2. *Cont.*

Pos.	Sample	Preparation	Reaction Conditions	Operation Temperature for Achieving 100% NH_3 Conversion/°C	N_2 Selectivity/%	Refs.
18	(10 wt.%)Cu/Al_2O_3	Impregnation, calcination, 600 °C, air, 24 h	1.14 vol.% NH_3, 8.21 vol.% O_2, He balance, WHSV 2240 mL h^{-1} g^{-1} * 1.14 vol.% NH_3, 8.21 vol.% O_2, He balance, WHSV 2240 mL h^{-1} g^{-1}	350 * 350	94 * 95	[62]
19	(10 wt.%)Cu/Al_2O_3	Impregnation, calcination, 600 °C, air, 3 h, * $Cu(CH_3COO)_2$ as precursor ** $Cu(NO_3)_2$ as precursor	0.1 vol.% NH_3, 10 vol.% O_2, He balance, GHSV 50,000 h^{-1}	* 350–400 ** 375–400	* >85 ** >95	[70]
20	(10 wt.%)Cu/Al_2O_3	Impregnation, calcination, 600 °C, air, 6 h	0.5 vol.% NH_3, 2.5 vol.% O_2, N_2 balance, WHSV 137,000–140,000 mL h^{-1} g^{-1} * 0.5 vol.% NH_3, 2.5 vol.% O_2, 10 vol.% CO_2, 5 vol.% H_2O, N_2 balance, WHSV 137,000–140,000 mL h^{-1} g^{-1}	450–600 * 600	>60 * >50	[111]
21	(10 wt.%)Cu/Al_2O_3	Impregnation, calcination, 600 °C, air, 12 h	0.5 vol.% NH_3, 2.5 vol.% O_2 Ar balance, WHSV 24,000 mL h^{-1} g^{-1}	425–500	>75	[112]
22	(10 wt.%)Cu/Al_2O_3 * (10 wt.%)Cu/Al_2O_3	Imprgnation, rotary evaporation, calcination, 500 °C, air, 2 h * Impregnation, rotary evaporation, 500 °C, H_2/N_2, 2 h; 0.05 vol.% NH_3, 5 vol.% O_2, N_2 balance	0.05 vol.% NH_3, 5 vol.% O_2 N_2 balance, GHSV 60,000 h^{-1}	330 * 300–330	not shown * not shown	[9]
23	(1.3 wt.%)Cu/Al_2O_3 * (1 wt.%)$Cu/CeO_x/Li_2O/Al_2O_3$	Impregnation, calcination, 350 °C, air, time not given; homogenous deposition precipitation, H_2 reduction, 400 °C, 2 h	2 vol.% NH_3, 2 vol.% O_2, Ar balance, GHSV 2500 h^{-1}	400 * 325–400	100 * 100	[76]
24	(3.4 wt.%)Cu/Al_2O_3	Impregnation, calcination, 450 °C, air, 5 h	0.54 vol.% NH_3, 8 vol.% O_2, He balance, WHSV 240 mL h^{-1} g^{-1}	400–450	not shown	[69]

Table 2. *Cont.*

Pos.	Sample	Preparation	Reaction Conditions	Operation Temperature for Achieving 100% NH_3 Conversion/°C	N_2 Selectivity/%	Refs.
25	(20 wt.%)Cu/Al_2O_3/monolith	Impregnation, calcination, 800 °C, air, 4 h	0.04 vol.% NH_3, 8.2 vol.% O_2, 1.3 vol.% CH_4, 3.9 vol.% CO_2, 4.1 vol.% CO, 2.9 vol.% H_2, GHSV 100,000 h^{-1}	400–500	0	[71]
26	(1 wt.%)PbO-(4.3 wt.%)Cu/Al_2O_3	Impregnation, calcination, 450 °C, air, time not shown	0.54 vol.% NH_3, 8 vol.% O_2, He balance, WHSV 800 mL h^{-1} g^{-1}	325	95	[68]
27	(1–2 wt.%)Cu/η-Al_2O_3	Impregnation, Rotary evaporator, calcination, 500 °C, air, 10 h; pre-treatment conditions: 20 vol.% O_2/He, 550 °C, 1 h	0.1 vol.% NH_3, 8 vol.% O_2, 3.5 vol.% H_2O, He balance, WHSV 250,000 mL h^{-1} g^{-1}	550	not shown	[75]
28	CuO/CNTs (carbon nanotubes, 9.85 wt.% Cu)	Impregnation, ultrasonic treatmnet, evaporation, 350 °C, He, 3 h	0.1 vol.% NH_3, 2 vol.% O_2, He balance, WHSV 60,000 mL h^{-1} g^{-1}	189–250	>98	[63]
29	Cu/graphene (2.57–3.42 wt.%)	Impregnation, ultrasonic treatment, 400 °C, N_2, 3 h, * $Cu(CH_3COO)_2$ H_2O as precursor ** $Cu(NO_3)_2 \cdot H_2O$ as precursor	0.05 vol.% NH_3, 1 vol.% O_2, N_2 balance, GHSV 35,000 h^{-1}	* 300 ** 250–300	* >80 ** >80	[72]
30	(5 wt.%)Ni/Al_2O_3	Impregnation, calcination, 800 °C, air, 8 h	0.1 vol.% NH_3, 18 vol.% O_2, N_2 balance, GHSV 61,000 h^{-1}	550–800	>55	[78]
31	(5 wt.%)Mn/Al_2O_3			300–800	>55	
32	(10.5 wt.%)$CuO/TiSnO_2$	Impregnation, calcination, 450 °C, air, 4 h	0.05 vol.% NH_3, 3 vol.% O_2, N_2 balance, WHSV 60,000 mL h^{-1} g^{-1}	300–400	>70	[85]
33	(5 wt.%)$CuO_x/La_2Ce_2O_7$	Impregnation, calcination, 600 °C, air, 1 h	0.05 vol.% NH_3, 5 vol.% O_2, N_2 balance, GHSV 20,000 h^{-1}	275–425	>80	[67]
34	(10 wt.%)Ce/(2 wt.%)V/TiO_2	Impregnation, calcination, 400 °C, air, 4 h; pre-treatment conditions: 8 vol.% O_2/N_2, 400 °C, 0.5 h	0.02 vol.% NH_3, 8 vol.% O_2, 6 vol.% H_2O, N_2 balance, GHSV 120,000 h^{-1}	300–350	>90	[95]
35	$Ce_{0.4}Zr_{0.6}O_2$	Surfactant-templated method, calcination, 550 °C, air, 3 h	0.1 vol.% NH_3, 10 vol.% O_2, He balance, GHSV 40,000 h^{-1}	360–380	>90	[93]

Table 2. *Cont.*

Pos.	Sample	Preparation	Reaction Conditions	Operation Temperature for Achieving 100% NH_3 Conversion/°C	N_2 Selectivity/%	Refs.
36	(6 wt.%)Cu-Ce-Zr n(Si)/n(Al) = 4	Sol-gel method, calcination, 450 °C, air, 3 h	0.1 vol.% NH_3, 10 vol.% O_2, He balance, GHSV 40,000 h^{-1}	230	>90	[97]
37	CuO-Fe_2O_3 n(Cu)/n(Fe) = 1:1	Sol-gel method, calcination, 500 °C, air, 4 h	0.08 vol.% NH_3, 5 vol.% O_2, Ar balance, GHSV 60,000 h^{-1}	225–300	>80	[87]
38	CuO-Fe_2O_3 n(Cu)/n(Fe) = 5:5	Sol-gel method, calcination, 400 °C, air, 4 h	0.08 vol.% NH_3, 5 vol.% O_2, Ar balance, GHSV 60,000 h^{-1}	250–300	>80	[86]
39	$CuFe_2O_4$ (8.59 wt.% Cu, 7.45 wt.% Fe)	Hard-template method, 600 °C, air, 6 h	0.1 vol.% NH_3, 0.2 vol.% O_2, He balance, GHSV 35,000 h^{-1}	350–600	>75	[88]
40	CuO-CeO_2 n(Cu)/n(Ce) = 6/4	Coprecipitation, calcination, 500 °C, air, 4 h	0.1 vol.% NH_3, 4 vol.% O_2, 12 vol.% H_2O, He balance, WHSV 92,000 mL h^{-1} g^{-1}	400	82	[99]
41	CuO-CeO_2 (10 wt.% Cu)	Surfactant templated method, 500 °C, air, 3 h	0.1 vol.% NH_3, 10 vol.% O_2, He balance, GHSV 40,000 h^{-1}	250–300	>90	[100]
42	(1 wt.%)Cu-PILC-Verm (Alumina pillared vermiculites)	Ion-exchange, calcination, 450 °C, air, 3 h	0.5 vol.% NH_3, 2.5 vol.% O_2, He balance, WHSV 24,000 mL h^{-1} g^{-1}	500–550	>95	[89]
43	(5.7 wt.%)Fe-PILC-Phlog (Alumina pillared phlogopite)			500–550	>70	
44	(0.59 wt.%)Cu-PCH (Porous clay heterostructures)	Ion-exchange, 450 °C, air, 3 h	0.5 vol.% NH_3, 2.5 vol.% O_2, He balance, WHSV 24,000 mL h^{-1} g^{-1}	500–550	>90	[53]
45	(1.43 wt.%)Cu-PCH (Porous clay heterostructures)			400–550	>90	[90]
46	Cu/attapulgite (5–10 wt.% Cu)	Impregnation, 400 °C, air, 4 h	0.005 vol.% NH_3, 4 vol.% O_2, N_2 balance, GHSV 150,000 h^{-1}	450–500	>75	[92]
47	natural manganese ore	Fluidization, 12 h	0.05 vol.% NH_3, 3 vol.% O_2, He balance, GHSV 15,000–80,000 h^{-1}	240	>70	[103]
48	MnO_2	Calcination, 400 °C, air, 2 h		210	>60	
49	Cu-Mn/TiO_2 n(Cu)/n(Mn) = 20/80	Impregnation, rotary evaporator, calcination, 550 °C, air, 2 h	0.06 vol.% NH_3, 6 vol.% O_2, N_2 balance, WHSV 200,000 mL h^{-1} g^{-1}	307	not shown	[104]

Table 2. *Cont.*

Pos.	Sample	Preparation	Reaction Conditions	Operation Temperature for Achieving 100% NH_3 Conversion/°C	N_2 Selectivity/%	Refs.
50	MnO_x-TiO_2 (27.8 wt.% Mn)	Sol-gel method, calcination, 500 °C, air, 4 h	0.05 vol.% NH_3, 5 vol.% O_2, He balance, WHSV 240,000 mL h^{-1} g^{-1}	200–350	>60	[106]
51	$SmMn_2O_5$	Organic solution combustion methods, 700 °C, air, 8 h	0.05 vol.% NH_3, 10 vol.% O_2, N_2 balance, WHSV 120,000 mL h^{-1} g^{-1}	175–250	>45	[108]
52	(5.0 wt.%)Nb_2O_5/$SmMn_2O_5$	Impregnation, 450 °C, air, 2 h		200–250	>60	
53	(30 wt.%)$SmMn_2O_5$/ Cu-SAPO	Grinding the mixture; * after hydrothermal aging treatment conditions: 21 vol.% O_2, 10 vol.% H_2O, N_2 balance, 800 °C, 5 h	0.05 vol.% NH_3, 21 vol.% O_2, N_2 balance, GHSV 100,000 h^{-1}	225–400 * 300–400	>20 * not shown	[109]
54	$La_xSr_{1-x}MnO_3$	Hydrothermal method, 400 °C, air, 2 h, post-treatment in 3 M HNO_3	0.05 vol.% NH_3, 3 vol.% O_2, N_2 balance, WHSV 120,000 mL h^{-1} g^{-1}	300–450	not shown	[110]

4. Conclusions and Future Perspectives

In this short mini-review, we have discussed recent trends, limits and opportunities offered by hydrotalcite-derived mixed metal oxides as opposed to the other transition metal-based catalysts applied in NH_3-SCO. Although there are relatively several catalytic systems proposed in the literature, at the same time, their systematic investigations and further improvement are scarce. Furthermore, there is a lack of systematic investigations of the reaction mechanisms. The mechanisms of NH_3-SCO have been explored mainly by the application of in situ DRIFTS and the indication of the characteristic intermediates of the imide, hydrazine or i-SCR mechanism.

Overall, based on our comparison, two transition metal-based catalytic systems can be selected for the preparation of the next-generation catalysts, i.e., the CuMgAl hydrotalcite-derived mixed metal oxides and Cu/Al_2O_3. The complete NH_3 conversion activity between 375–650 °C and N_2 selectivity above 70% were reached over hydrotalcite-derived mixed metal oxides. Similarly, Cu/Al_2O_3 being the most frequently studied catalyst reached full NH_3 conversion at 350–500 °C with N_2 selectivity above 75%. Our revision is further supported by our previous study [111], where the activity and N_2 selectivity in NH_3-SCO over hydrotalcite-derived CuMgAl (n(Cu)/n(Mg)/n(Al) = 8/63/29, mol.%) mixed metal oxides and (10 wt.%)Cu/Al_2O_3 were tested under $NH_3/O_2/CO_2/H_2O/N_2$ conditions by applying ca. 6.5–6.7 g of catalysts. The mixture of the highly dispersed easily reducible copper oxide and bulk copper oxide species allowed for enhanced activity, N_2 selectivity and stability. Still, further work is needed on the systematic catalysts' chemical and phase optimization and catalyst tests, including investigations under more applied reaction conditions concerning either reaction mixture composition (NH_3 concentration of about 100 ppm with O_2 concentrations of about 10 vol.%; in the presence of CO_x, SO_x and H_2O) or temperature (up to 600–700 °C), should follow. Furthermore, thermal stability should be tested, as well as catalyst poisoning via the typical components of the lubricating oil for diesel engines (e.g., Ca, Zn, P and S species). A comprehensive understanding of the involved active species, e.g., through operando technologies under realistic working conditions, could facilitate a knowledge-based catalyst optimization to obtain desired NH_3 slip catalysts.

Author Contributions: Conceptualization, M.J.; writing-original draft preparation, M.J. and. A.M.R.; writing—review and editing, M.J.; supervision, M.J.; project administration, M.J. All authors have read and agreed to the published version of the manuscript.

Funding: This research was funded by DFG Research Grant JA 2998/2-1.

Institutional Review Board Statement: Not applicable.

Informed Consent Statement: Not applicable.

Data Availability Statement: Not applicable.

Acknowledgments: We acknowledge support from the German Research Foundation (DFG) and Leipzig University within the program of Open Access Publishing.

Conflicts of Interest: The authors declare no conflict of interest.

References

1. European Environment Agency. Available online: https://www.eea.europa.eu/publications/national-emission-reduction-commitments-directive (accessed on 30 May 2022).
2. Arasu, P.T.; Khalaf, A.L.; Aziz, S.H.A.; Yaacob, M.H.; Noor, A.S.M. Optical fiber based ammonia gas sensor with carbon nanotubes sensing enhancement. In Proceedings of the 2017 IEEE Region 10 Symposium (TENSYMP), Cochin, India, 14–16 July 2017; pp. 1–4.
3. Chmielarz, L.; Jabłońska, M. Advances in selective catalytic oxidation of ammonia to dinitrogen: A review. *RSC Adv.* **2015**, *5*, 43408–43431. [CrossRef]
4. Jabłońska, M.; Palkovits, R. Copper based catalysts for the selective ammonia oxidation into nitrogen and water vapour-Recent trends and open challenges. *Appl. Catal. B Environ.* **2016**, *181*, 332–351. [CrossRef]

5. Jabłońska, M. Progress on noble metal-based catalysts dedicated to the selective catalytic ammonia oxidation into nitrogen and water vapor (NH_3-SCO). *Molecules* **2021**, *26*, 6461. [CrossRef] [PubMed]
6. Jabłońska, M. Progress on selective catalytic ammonia oxidation (NH_3-SCO) over Cu-containing zeolite-based catalysts. *ChemCatChem* **2002**, *12*, 4490–4500. [CrossRef]
7. Torp, T.K.; Hansen, B.B.; Vennestrøm, P.N.R.; Janssens, T.V.W.; Jensen, A.D. Modeling and optimization of multi-functional ammonia slip catalysts for diesel exhaust aftertreatment. *Emiss. Control Sci. Technol.* **2021**, *7*, 7–25. [CrossRef]
8. Wang, F.; Ma, J.; He, G.; Chen, M.; Zhang, C.; He, H. Nanosize effect of Al_2O_3 in Ag/Al_2O_3 catalyst for the selective catalytic oxidation of ammonia. *ACS Catal.* **2018**, *8*, 2670–2682. [CrossRef]
9. Lan, T.; Deng, J.; Zhang, X.; Wang, F.; Liu, X.; Cheng, D.; Zhang, D. Unraveling the promotion effects of dynamically constructed CuO_x-OH interfacial sites in the selective catalytic oxidation of ammonia. *ACS Catal.* **2022**, *12*, 3955–3964. [CrossRef]
10. Gao, F.; Liu, Y.; Sani, Z.; Tang, X.; Yi, H.; Zhao, S.; Yu, Q.; Zhou, Y. Advances in selective catalytic oxidation of ammonia (NH_3-SCO) to dinitrogen in excess oxygen: A review on typical catalysts, catalytic performances and reaction mechanisms. *J. Environ. Chem. Eng.* **2020**, *9*, 104575–104595. [CrossRef]
11. Rives, V.; Ulibarri, M.A. Layered double hydroxides (LDH) intercalated with metal coordination compounds and oxometalates. *Coord. Chem. Rev.* **1999**, *181*, 61–120. [CrossRef]
12. Evans, D.G.; Slade, R.C.T. Structural aspects of layered double hydroxides. In *Layered Double Hydroxides*; Springer: Berlin/Heidelberg, Germany, 2006; pp. 1–87.
13. Basile, F.; Fornasari, G.; Gazzano, M.; Vaccari, A. Synthesis and thermal evolution of hydrotalcite-type compounds containing noble metals. *Appl. Clay Sci.* **2000**, *16*, 185–200. [CrossRef]
14. Centi, G.; Perathoner, S. Catalysis by layered materials: A review. *Microporous Mesoporous Mater.* **2008**, *107*, 3–15. [CrossRef]
15. Kannan, S. Catalytic applications of hydrotalcite-like materials and their derived forms. *Catal. Surv. Asia* **2006**, *10*, 117–137. [CrossRef]
16. Jabłońska, M.; Palkovits, R. Nitrogen oxide removal over hydrotalcite-derived mixed metal oxides. *Catal. Sci. Technol.* **2016**, *6*, 49–72. [CrossRef]
17. Jabłońska, M.; Palkovits, R. It is no laughing matter: Nitrous oxide formation in diesel engines and advances in its abatement over rhodium-based catalysts. *Catal. Sci. Technol.* **2016**, *6*, 7671–7687. [CrossRef]
18. Schmidt-Szałowski, K.; Krawczyk, K.; Petryk, J. The properties of cobalt oxide catalyst for ammonia oxidation. *Appl. Catal. A Gen.* **1998**, *175*, 147–157. [CrossRef]
19. Petryk, J.; Kołakowska, E. Cobalt oxide catalysts for ammonia oxidation activated with cerium and lanthanum. *Appl. Catal. B Environ.* **2000**, *24*, 121–128. [CrossRef]
20. Escandón, L.S.; Ordóñez, S.; Díez, F.V.; Sastre, H. Ammonia oxidation over conventional combustion catalysts. *React. Kinet. Catal. Lett.* **2002**, *76*, 61–68. [CrossRef]
21. Zakharchenko, N.I. Catalytic Properties of the Fe_2O_3-MnO System for Ammonia Oxidation. *Kinet. Catal.* **2001**, *42*, 679–685. [CrossRef]
22. Sadykov, V.A.; Isupova, L.A.; Zolotarskii, I.A.; Bobrova, L.N.; Noskov, A.S.; Parmon, V.N.; Brushtein, E.A.; Telyatnikova, T.V.; Chernyshev, V.I.; Lunin, V.V. Oxide catalysts for ammonia oxidation in nitric acid production: Properties and perspectives. *Appl. Catal. A Gen.* **2000**, *204*, 59–87. [CrossRef]
23. Noskov, A.S.; Zolotarskii, I.A.; Pokrovskaya, S.A.; Korotkikh, V.N.; Slavinskaya, E.M.; Mokrinskii, V.V.; Kashkin, V.N. Ammonia oxidation into nitrous oxide over Mn/Bi/Al catalyst: I. Single cooling tube experiments. *Chem. Eng. J.* **2003**, *91*, 235–242. [CrossRef]
24. Slavinskaya, E.M.; Veniaminov, S.A.; Notté, P.; Ivanova, A.S.; Boronin, A.I.; Chesalov, Y.A.; Polukhina, I.A.; Noskov, A.S. Studies of the mechanism of ammonia oxidation into nitrous oxide over $MnBiO/\alpha$-Al_2O_3 catalyst. *J. Catal.* **2004**, *222*, 129–142. [CrossRef]
25. Cavani, F.; Trifiro, F.; Vaccari, A. Hydrotalcite-type anionic clays: Preparation, properties and applications. *Catal. Today* **1991**, *11*, 173–301. [CrossRef]
26. Yan, K.; Wu, G.; Jin, W. Recent advances in the synthesis of layered, double-hydroxide-Based materials and their applications in hydrogen and oxygen evolution. *Energy Technol.* **2016**, *4*, 354–368. [CrossRef]
27. Newman, S.P.; Jones, W.; O'Connor, P.; Stamires, D.N. Synthesis of the 3R 2 polytype of a hydrotalcite-like mineral. *J. Mater. Chem.* **2002**, *12*, 153–155. [CrossRef]
28. Jabłońska, M.; Chmielarz, L.; Węgrzyn, A.; Guzik, K.; Piwowarska, Z.; Witkowski, S.; Walton, R.I.; Dunne, P.W.; Kovanda, F. Thermal transformations of Cu-Mg (Zn)-Al(Fe) hydrotalcite-like materials into metal oxide systems and their catalytic activity in selective oxidation of ammonia to dinitrogen. *J. Therm. Anal. Calorim.* **2013**, *114*, 731–747. [CrossRef]
29. Trombetta, M.; Ramis, G.; Busca, G.; Montanari, B.; Vaccari, A. Ammonia adsorption and oxidation on Cu/Mg/Al mixed oxide catalysts prepared via hydrotalcite-type precursors. *Langmuir* **1997**, *13*, 4628–4637. [CrossRef]
30. Chmielarz, L.; Kuśtrowski, P.; Rafalska-Łasocha, A.; Dziembaj, R. Selective oxidation of ammonia to nitrogen on transition metal containing mixed metal oxides. *Appl. Catal. B Environ.* **2005**, *58*, 235–244. [CrossRef]
31. Chmielarz, L.; Węgrzyn, A.; Wojciechowska, M.; Witkowski, S.; Michalik, M. Selective catalytic oxidation (SCO) of ammonia to nitrogen over hydrotalcite originated Mg-Cu-Fe mixed metal oxides. *Catal. Lett.* **2011**, *141*, 1345–1354. [CrossRef]
32. Górecka, S.; Pacultová, K.; Górecki, K.; Smýkalová, A.; Pamin, K.; Obalová, L. Cu-Mg-Fe-O-(Ce) complex oxides as catalysts of selective catalytic oxidation of ammonia to dinitrogen (NH_3-SCO). *Catalysts* **2020**, *10*, 153. [CrossRef]

33. Chmielarz, L.; Jabłońska, M.; Strumiński, A.; Piwowarska, Z.; Węgrzyn, A.; Witkowski, S.; Michalik, M. Selective catalytic oxidation of ammonia to nitrogen over Mg-Al, Cu-Mg-Al and Fe-Mg-Al mixed metal oxides doped with noble metals. *Appl. Catal. B Environ.* **2013**, *130*, 152–162. [CrossRef]
34. Jabłońska, M.; Nocuń, M.; Gołąbek, K.; Palkovits, R. Effect of preparation procedures on catalytic activity and selectivity of copper-based mixed oxides in selective catalytic oxidation of ammonia into nitrogen and water vapour. *Appl. Surf. Sci.* **2017**, *423*, 498–508. [CrossRef]
35. Basąg, S.; Piwowarska, Z.; Kowalczyk, A.; Węgrzyn, A.; Baran, R.; Gil, B.; Michalik, M.; Chmielarz, L. Cu-Mg-Al hydrotalcite-like materials as precursors of effective catalysts for selective oxidation of ammonia to dinitrogen—The influence of Mg/Al ratio and calcination temperature. *Appl. Clay Sci.* **2016**, *129*, 122–130. [CrossRef]
36. Jabłońska, M.; Nothdurft, K.; Nocuń, M.; Girman, V.; Palkovits, R. Redox-performance correlations in Ag-Cu-Mg-Al, Ce-Cu-Mg-Al, and Ga-Cu-Mg-Al hydrotalcite derived mixed metal oxides. *Appl. Catal. B Environ.* **2017**, *207*, 385–396. [CrossRef]
37. Górecka, S.; Pacultová, K.; Smýkalová, A.; Fridrichová, D.; Górecki, K.; Rokicińska, A.; Kuśtrowski, P.; Žebrák, R.; Obalová, L. Role of the Cu content and Ce activating effect on catalytic performance of Cu-Mg-Al and Ce/Cu-Mg-Al oxides in ammonia selective catalytic oxidation. *Appl. Surf. Sci.* **2022**, *573*, 151540–151555. [CrossRef]
38. Basąg, S.; Kocoł, K.; Piwowarska, Z.; Rutkowska, M.; Baran, R.; Chmielarz, L. Activating effect of cerium in hydrotalcite derived Cu-Mg-Al catalysts for selective ammonia oxidation and the selective reduction of NO with ammonia. *React. Kinet. Mech. Catal.* **2017**, *121*, 225–240. [CrossRef]
39. Górecka, S.; Pacultová, K.; Fridrichová, D.; Górecki, K.; Bílková, T.; Žebrák, R.; Obalová, L. Catalytic oxidation of ammonia over cerium-modified copper aluminium zinc mixed oxides. *Materials* **2021**, *14*, 6581. [CrossRef]
40. Ludvíková, J.; Jabłońska, M.; Jirátová, K.; Chmielarz, L.; Balabánová, J.; Kovanda, F.; Obalová, L. Co-Mn-Al mixed oxides as catalysts for ammonia oxidation to N_2O. *Res. Chem. Intermed.* **2016**, *42*, 2669–2690. [CrossRef]
41. Il'Chenko, N.I.; Golodets, G.I. Catalytic oxidation of ammonia: I. Reaction kinetics and mechanism. *J. Catal.* **1975**, *39*, 57–72. [CrossRef]
42. Il'chenko, N.I.; Golodets, G.I. Catalytic oxidation of ammonia: II. Relationship between catalytic properties of substances and surface oxygen bond energy. General regularities in catalytic oxidation of ammonia and organic substances. *J. Catal.* **1975**, *39*, 73–86. [CrossRef]
43. Il'chenko, N.I. Catalytic oxidation of ammonia. *Russ. Chem. Rev.* **1976**, *45*, 1119. [CrossRef]
44. Hinokuma, S.; Shimanoe, H.; Matsuki, S.; Kawano, M.; Kawabata, Y.; Machida, M. Catalytic activity and selectivities of metal oxides and Pt/Al_2O_3 for NH_3 combustion. *Chem. Lett.* **2016**, *45*, 179–181. [CrossRef]
45. Gandhi, H.S.; Shelef, M. Selectivity for nitrogen formation in NH_3 oxidation in wet and dry systems over mixed molybdenum oxides. *J. Catal.* **1975**, *40*, 312–317. [CrossRef]
46. Chen, J.P.; Yang, R.T. Role of WO_3 in mixed V_2O_5-WO_3/TiO_2 catalysts for selective catalytic reduction of nitric oxide with ammonia. *Appl. Catal. A Gen.* **1992**, *80*, 135–148. [CrossRef]
47. Cavani, F.; Trifiro, F. Oxidation of NH_3 on V/Ti oxide based catalysts prepared by precipitation. *Catal. Today* **1989**, *4*, 253–265. [CrossRef]
48. Biermann, J.J.; Janssen, F.J. Low temperature isotopic exchange of molecular oxygen via the reaction of NO, NH_3 and O_2 over supported vanadia and molybdena catalysts. *Catal. Lett.* **1989**, *2*, 385–393. [CrossRef]
49. Nova, I.; Dall'Acqua, L.; Lietti, L.; Giamello, E.; Forzatti, P. Study of thermal deactivation of a de-NO_x commercial catalyst. *Appl. Catal. B Environ.* **2001**, *35*, 31–42. [CrossRef]
50. Due-Hansen, J.; Kustov, A.L.; Christensen, C.H.; Fehrmann, R. Impact of support and potassium-poisoning on the V_2O_5-WO_3/ZrO_2 catalyst performance in ammonia oxidation. *Catal. Commun.* **2009**, *10*, 803–806. [CrossRef]
51. Ueshima, M.; Sano, K.; Ikeda, M.; Yoshino, K.; Okamura, J. New technology for selective catalytic oxidation of ammonia to nitrogen. *Res. Chem. Intermed.* **1998**, *24*, 133–141. [CrossRef]
52. Sazonova, N.N.; Simakov, A.V.; Nikoro, T.A.; Barannik, G.B.; Lyakhova, V.F.; Zheivot, V.I.; Ismagilov, Z.R.; Veringa, H. Selective catalytic oxidation of ammonia to nitrogen. *React. Kinet. Catal. Lett.* **1996**, *57*, 71–79. [CrossRef]
53. Liu, W.; Long, Y.; Liu, S.; Zhou, Y.; Tong, X.; Yin, Y.; Li, X.; Hu, K.; Hu, J. Promotional effect of Ce in NH_3-SCO and NH_3-SCR reactions over Cu-Ce/SCR catalysts. *J. Ind. Eng. Chem.* **2021**, *107*, 197–206. [CrossRef]
54. Liu, W.; Long, Y.; Tong, X.; Yin, Y.; Li, X.; Hu, J. Transition metals modified commercial SCR catalysts as efficient catalysts in NH_3-SCO and NH_3-SCR reactions. *Mol. Catal.* **2021**, *515*, 111888–111897. [CrossRef]
55. Yuan, R.-M.; Fu, G.; Xu, X.; Wan, H.-L. Mechanisms for selective catalytic oxidation of ammonia over vanadium oxides. *J. Phys. Chem. C* **2011**, *115*, 21218–21229. [CrossRef]
56. Liu, Y.; Hu, Q.; Ma, D.; Liu, X.; You, Z.; Qiu, G.; Lv, X. Periodic DFT study on the adsorption and deoxygenation process of NH_3 on V_2O_5 (001) surface. *JOM* **2022**, *74*, 1870–1877. [CrossRef]
57. Carley, A.F.; Davies, P.R.; Roberts, M.W. An STM-XPS study of ammonia oxidation: The molecular architecture of chemisorbed imide 'strings' at Cu (110) surfaces. *Chem. Commun.* **1998**, *17*, 1793–1794. [CrossRef]
58. Mayer, R.W.; Hävecker, M.; Knop-Gericke, A.; Schlögl, R. Investigation of ammonia oxidation over copper with in situ NEXAFS in the soft X-ray range: Influence of pressure on the catalyst performance. *Catal. Lett.* **2001**, *74*, 115–119. [CrossRef]

59. Mayer, R.W.; Melzer, M.; Hävecker, M.; Knop-Gericke, A.; Urban, J.; Freund, H.-J.; Schlögl, R. Comparison of oxidized polycrystalline copper foil with small deposited copper clusters in their behavior in ammonia oxidation: An investigation by means of in situ NEXAFS spectroscopy in the soft X-ray range. *Catal. Lett.* **2003**, *86*, 245–260. [CrossRef]
60. Hirabayashi, S.; Ichihashi, M. Gas-phase reactions of copper oxide cluster cations with ammonia: Selective catalytic oxidation to nitrogen and water molecules. *J. Phys. Chem. A* **2018**, *122*, 4801–4807. [CrossRef]
61. Gang, L.; Van Grondelle, J.; Anderson, B.G.; Van Santen, R.A. Selective low temperature NH_3 oxidation to N_2 on copper-based catalysts. *J. Catal.* **1999**, *186*, 100–109. [CrossRef]
62. Gang, L.; Anderson, B.G.; Van Grondelle, J.; Van Santen, R.A. NH_3 oxidation to nitrogen and water at low temperatures using supported transition metal catalysts. *Catal. Today* **2000**, *61*, 179–185. [CrossRef]
63. Song, S.; Jiang, S. Selective catalytic oxidation of ammonia to nitrogen over CuO/CNTs: The promoting effect of the defects of CNTs on the catalytic activity and selectivity. *Appl. Catal. B Environ.* **2012**, *117*, 346–350. [CrossRef]
64. Hung, C.-M. Synthesis, characterization and performance of CuO/La_2O_3 composite catalyst for ammonia catalytic oxidation. *Powder Technol.* **2009**, *196*, 56–61. [CrossRef]
65. He, S.; Zhang, C.; Yang, M.; Zhang, Y.; Xu, W.; Cao, N.; He, H. Selective catalytic oxidation of ammonia from MAP decomposition. *Sep. Purif. Technol.* **2007**, *58*, 173–178. [CrossRef]
66. Kaddouri, A.; Dupont, N.; Gélin, P.; Auroux, A. Selective oxidation of gas phase ammonia over copper chromites catalysts prepared by the sol-gel process. *Catal. Commun.* **2011**, *15*, 32–36. [CrossRef]
67. Kong, X.; Li, Z.; Shao, Y.; Ren, X.; Li, K.; Wu, H.; Lv, C.; Lv, C.; Zhu, S. Modulate the superficial structure of $La_2Ce_2O_7$ catalyst with anchoring CuO_x species for the selective catalytic oxidation of NH_3. *J. Mater. Sci. Technol.* **2022**, *111*, 1–8. [CrossRef]
68. Curtin, T.; O'Regan, F.; Deconinck, C.; Knüttle, N.; Hodnett, B.K. The catalytic oxidation of ammonia: Influence of water and sulfur on selectivity to nitrogen over promoted copper oxide/alumina catalysts. *Catal. Today* **2000**, *55*, 189–195. [CrossRef]
69. Lenihan, S.; Curtin, T. The selective oxidation of ammonia using copper-based catalysts: The effects of water. *Catal. Today* **2009**, *145*, 85–89. [CrossRef]
70. Liang, C.; Li, X.; Qu, Z.; Tade, M.; Liu, S. The role of copper species on Cu/γ-Al_2O_3 catalysts for NH_3-SCO reaction. *Appl. Surf. Sci.* **2012**, *258*, 3738–3743. [CrossRef]
71. Kušar, H.M.J.; Ersson, A.G.; Vosecký, M.; Järås, S.G. Selective catalytic oxidation of NH_3 to N_2 for catalytic combustion of low heating value gas under lean/rich conditions. *Appl. Catal. B Environ.* **2005**, *58*, 25–32. [CrossRef]
72. Li, J.; Tang, X.; Yi, H.; Yu, Q.; Gao, F.; Zhang, R.; Li, C.; Chu, C. Effects of copper-precursors on the catalytic activity of Cu/graphene catalysts for the selective catalytic oxidation of ammonia. *Appl. Surf. Sci.* **2017**, *412*, 37–44. [CrossRef]
73. Darvell, L.I.; Heiskanen, K.; Jones, J.M.; Ross, A.B.; Simell, P.; Williams, A. An investigation of alumina-supported catalysts for the selective catalytic oxidation of ammonia in biomass gasification. *Catal. Today* **2003**, *81*, 681–692. [CrossRef]
74. Jones, J.M.; Pourkashanian, M.; Williams, A.; Backreedy, R.I.; Darvell, L.I.; Simell, P.; Heiskanen, K.; Kilpinen, P. The selective oxidation of ammonia over alumina supported catalysts-experiments and modelling. *Appl. Catal. B Environ.* **2005**, *60*, 139–146. [CrossRef]
75. Jraba, N.; Makhlouf, T.; Delahay, G.; Tounsi, H. Catalytic activity of Cu/η-Al_2O_3 catalysts prepared from aluminum scraps in the NH_3-SCO and in the NH_3-SCR of NO. *Environ. Sci. Pollut. Res.* **2022**, *29*, 9053–9064. [CrossRef]
76. Lippits, M.J.; Gluhoi, A.C.; Nieuwenhuys, B.E. A comparative study of the selective oxidation of NH_3 to N_2 over gold, silver and copper catalysts and the effect of addition of Li_2O and CeO_x. *Catal. Today* **2008**, *137*, 446–452. [CrossRef]
77. Machida, M.; Tokudome, Y.; Maeda, A.; Sato, T.; Yoshida, H.; Ohyama, J.; Fujii, K.; Ishikawa, N. A comparative study of various transition metal overlayer catalysts for low-temperature NH_3 oxidation under dry and wet conditions. *Catal. Today* **2022**, *384*, 70–75. [CrossRef]
78. Amblard, M.; Burch, R.; Southward, B.W.L. The selective conversion of ammonia to nitrogen on metal oxide catalysts under strongly oxidising conditions. *Appl. Catal. B Environ.* **1999**, *22*, 159–166.
79. Nassos, S.; Svensson, E.E.; Nilsson, M.; Boutonnet, M.; Järås, S. Microemulsion-prepared Ni catalysts supported on cerium-lanthanum oxide for the selective catalytic oxidation of ammonia in gasified biomass. *Appl. Catal. B Environ.* **2006**, *64*, 96–102. [CrossRef]
80. Nassos, S.; Svensson, E.E.; Boutonnet, M.; Järås, S.G. The influence of Ni load and support material on catalysts for the selective catalytic oxidation of ammonia in gasified biomass. *Appl. Catal. B Environ.* **2007**, *74*, 92–102. [CrossRef]
81. Wang, W.Q.; Tang, X.L.; Yi, H.H.; Hu, J.L. A Comparative study of the selective oxidation of NH_3 to N_2 over transition metal catalysts. *Adv. Mater. Res.* **2013**, *798*, 239–244.
82. Jabłońska, M. Selective catalytic oxidation of ammonia into nitrogen and water vapour over transition metals modified Al_2O_3, TiO_2 and ZrO_2. *Chem. Pap.* **2015**, *69*, 1141–1155. [CrossRef]
83. Duan, K.; Tang, X.; Yi, H.; Zhang, Y.; Ning, P. Comparative study on low temperature selective catalytic oxidation of ammonia over transition metals supported on TiO_2. In Proceedings of the 2010 International Conference on Management and Service Science, Wuhan, China, 24–26 August 2010; pp. 1–4.
84. Jabłońska, M.; Ciptonugroho, W.; Góra-Marek, K.; Al-Shaal, M.G.; Palkovits, R. Preparation, characterization and catalytic performance of Ag-modified mesoporous TiO_2 in low-temperature selective ammonia oxidation into nitrogen and water vapour. *Microporous Mesoporous Mater.* **2017**, *245*, 31–44. [CrossRef]

85. Ge, S.; Liu, X.; Liu, J.; Liu, H.; Liu, H.; Chen, X.; Wang, G.; Chen, J.; Zhang, G.; Zhang, Y.; et al. Synthesis of $Ti_xSn_{1-x}O_2$ mixed metal oxide for copper catalysts as high-efficiency NH_3 selective catalytic oxidation. *Fuel* **2022**, *314*, 123061–123071. [CrossRef]
86. Zhang, Q.; Wang, H.; Ning, P.; Song, Z.; Liu, X.; Duan, Y. In situ DRIFTS studies on CuO-Fe_2O_3 catalysts for low temperature selective catalytic oxidation of ammonia to nitrogen. *Appl. Surf. Sci.* **2017**, *419*, 733–743. [CrossRef]
87. Wang, H.; Zhang, Q.; Zhang, T.; Wang, J.; Wei, G.; Liu, M.; Ning, P. Structural tuning and NH_3-SCO performance optimization of CuO-Fe_2O_3 catalysts by impact of thermal treatment. *Appl. Surf. Sci.* **2019**, *485*, 81–91. [CrossRef]
88. Yue, W.; Zhang, R.; Liu, N.; Chen, B. Selective catalytic oxidation of ammonia to nitrogen over orderly mesoporous $CuFe_2O_4$ with high specific surface area. *Chin. Sci. Bull.* **2014**, *59*, 3980–3986. [CrossRef]
89. Chmielarz, L.; Kuśtrowski, P.; Piwowarska, Z.; Michalik, M.; Dudek, B.; Dziembaj, R. Natural micas intercalated with Al_2O_3 and modified with transition metals as catalysts of the selective oxidation of ammonia to nitrogen. *Top. Catal.* **2009**, *52*, 1017–1022. [CrossRef]
90. Chmielarz, L.; Kuśtrowski, P.; Drozdek, M.; Dziembaj, R.; Cool, P.; Vansant, E.F. Selective catalytic oxidation of ammonia into nitrogen over PCH modified with copper and iron species. *Catal. Today* **2006**, *114*, 319–325. [CrossRef]
91. Chmielarz, L.; Kuśtrowski, P.; Dziembaj, R.; Cool, P.; Vansant, E.F. Selective catalytic reduction of NO with ammonia over porous clay heterostructures modified with copper and iron species. *Catal. Today* **2007**, *119*, 181–186. [CrossRef]
92. Chen, C.; Cao, Y.; Liu, S.; Chen, J.; Jia, W. The catalytic properties of Cu modified attapulgite in NH_3-SCO and NH_3-SCR reactions. *Appl. Surf. Sci.* **2019**, *480*, 537–547. [CrossRef]
93. Wang, Z.; Qu, Z.; Quan, X.; Wang, H. Selective catalytic oxidation of ammonia to nitrogen over ceria-zirconia mixed oxides. *Appl. Catal. A Gen.* **2012**, *411*, 131–138. [CrossRef]
94. Lee, S.M.; Lee, H.H.; Hong, S.C. Influence of calcination temperature on Ce/TiO_2 catalysis of selective catalytic oxidation of NH_3 to N_2. *Appl. Catal. A Gen.* **2014**, *470*, 189–198. [CrossRef]
95. Lee, S.M.; Hong, S.C. Promotional effect of vanadium on the selective catalytic oxidation of NH_3 to N_2 over Ce/V/TiO_2 catalyst. *Appl. Catal. B Environ.* **2015**, *163*, 30–39. [CrossRef]
96. Chen, W.; Ma, Y.; Qu, Z.; Liu, Q.; Huang, W.; Hu, X.; Yan, N. Mechanism of the selective catalytic oxidation of slip ammonia over Ru-modified Ce-Zr complexes determined by in situ diffuse reflectance infrared Fourier transform spectroscopy. *Environ. Sci. Technol.* **2014**, *48*, 12199–12205. [CrossRef]
97. Qu, Z.; Wang, Z.; Zhang, X.; Wang, H. Role of different coordinated Cu and reactive oxygen species on the highly active Cu-Ce-Zr mixed oxides in NH_3-SCO: A combined in situ EPR and O_2-TPD approach. *Catal. Sci. Technol.* **2016**, *6*, 4491–4502. [CrossRef]
98. Zhang, X.; Wang, H.; Wang, Z.; Qu, Z. Adsorption and surface reaction pathway of NH_3 selective catalytic oxidation over different Cu-Ce-Zr catalysts. *Appl. Surf. Sci.* **2018**, *447*, 40–48. [CrossRef]
99. Lou, J.-C.; Hung, C.-M.; Yang, S.-F. Selective catalytic oxidation of ammonia over copper-cerium composite catalyst. *J. Air Waste Manag. Assoc.* **2004**, *54*, 68–76. [CrossRef]
100. Wang, Z.; Qu, Z.; Quan, X.; Li, Z.; Wang, H.; Fan, R. Selective catalytic oxidation of ammonia to nitrogen over CuO-CeO_2 mixed oxides prepared by surfactant-templated method. *Appl. Catal. B Environ.* **2013**, *134*, 153–166. [CrossRef]
101. Hung, C.-M. Catalytic decomposition of ammonia over bimetallic CuO/CeO_2 nanoparticle catalyst. *Aerosol Air Qual. Res.* **2008**, *8*, 447–458. [CrossRef]
102. Hung, C.-M. Selective catalytic oxidation of ammonia to nitrogen on CuO-CeO_2 bimetallic oxide catalysts. *Aerosol Air Qual. Res.* **2006**, *6*, 150–169. [CrossRef]
103. Lee, J.Y.; Kim, S.B.; Hong, S.C. Characterization and reactivity of natural manganese ore catalysts in the selective catalytic oxidation of ammonia to nitrogen. *Chemosphere* **2003**, *50*, 1115–1122. [CrossRef]
104. Wöllner, A.; Lange, F.; Schmelz, H.; Knözinger, H. Characterization of mixed copper-manganese oxides supported on titania catalysts for selective oxidation of ammonia. *Appl. Catal. A Gen.* **1993**, *94*, 181–203. [CrossRef]
105. Kaijiao, D.; Xiaolong, T.; Honnghong, Y.; Ping, N.; Lida, W. Rare earth oxide modified Cu-Mn compounds supported on TiO_2 catalysts for low temperature selective catalytic oxidation of ammonia and in lean oxygen. *J. Rare Earths* **2010**, *28*, 338–342.
106. Song, D.; Shao, X.; Yuan, M.; Wang, L.; Zhan, W.; Guo, Y.; Guo, Y.; Lu, G. Selective catalytic oxidation of ammonia over MnO_x-TiO_2 mixed oxides. *RSC Adv.* **2016**, *6*, 88117–88125. [CrossRef]
107. Long, R.Q.; Yang, R.T. Selective catalytic oxidation of ammonia to nitrogen over Fe_2O_3-TiO_2 prepared with a sol-gel method. *J. Catal.* **2002**, *207*, 158–165. [CrossRef]
108. Chen, Y.; Chen, X.; Ma, X.; Tang, Y.; Zhao, Y.; Zhang, A.; Wang, C.; Du, C.; Shan, B. Selective catalytic oxidation of ammonia over AMn_2O_5 (A = Sm, Y, Gd) and reaction selectivity promotion through Nb decoration. *J. Catal.* **2021**, *402*, 10–21. [CrossRef]
109. Dong, A.; Yang, Z.; Wang, W. Mixed catalyst $SmMn_2O_5$/Cu-SAPO-34 for NH_3-selective catalytic oxidation. *ACS Omega* **2022**, *7*, 8633–8639. [CrossRef]
110. Wang, D.; Peng, Y.; Yang, Q.; Xiong, S.; Li, J.; Crittenden, J. Performance of modified La_xSr_{1-x} MnO_3 perovskite catalysts for NH_3 oxidation: TPD, DFT, and kinetic studies. *Environ. Sci. Technol.* **2018**, *52*, 7443–7449. [CrossRef]
111. Jabłońska, M.; Wolkenar, B.; Beale, A.M.; Pischinger, S.; Palkovits, R. Comparison of Cu-Mg-Al-O_x and Cu/Al_2O_3 in selective catalytic oxidation of ammonia (NH_3-SCO). *Catal. Commun.* **2018**, *110*, 5–9. [CrossRef]
112. Jabłońska, M.; Beale, A.M.; Nocuń, M.; Palkovits, R. Ag-Cu based catalysts for the selective ammonia oxidation into nitrogen and water vapour. *Appl. Catal. B Environ.* **2018**, *232*, 275–287. [CrossRef]